Identification and Characterization of a Novel Ethylene Inducing Substance in Tomato

Dissertation

der Mathematisch-Naturwissenschaftlichen Fakultät
der Eberhard Karls Universität Tübingen
zur Erlangung des Grades eines
Doktors der Naturwissenschaften
(Dr. rer. nat.)

vorgelegt von
Martin Gebhard Boehme
aus Leutkirch im Allgäu

Tübingen
2023

Gedruckt mit Genehmigung der Mathematisch-Naturwissenschaftlichen Fakultät der Eberhard Karls Universität Tübingen.

Tag der müdlichen Prüfung:	21.04.2023
Dekan:	Prof. Dr. Thilo Stehle
1. Berichterstatter:	Prof. Dr. Thorsten Nürnberger
2. Berichterstatter:	Prof. Dr. Stephanie Grond

Acknowledgements

Diese Arbeit waere nicht ohne die Unterstuezung von zahlreichen Kollegen und Freunden zustande gekommen. An dieser Stelle moechte ich deshalb meinen Dank aussprechen.

Prof. Dr. Thorsten Nuernberger, fuer die Moeglichkeit diese Dissertation durchzufuehren und fuer seine Anleitung waehrend dieser Zeit.

Prof. Dr. Stephanie Grond, fuer Rat, Unterstuetzung mit Laborequipment und den Beistand seit meiner Bachelorarbeit.

Dr. Andrea Gust, fuer gute Ideen und Zuspruch als Teil meines TAC-Committees.

Mein besonderer Dank gilt ausserdem den Mitgliedern der Pruefungskomission.

Den Kollegen der Arbeitsgruppen Nuernberger und Grond, vor allem Rory fuer das geduldige Beantworten meiner Fragen und den tollen Schachduellen, Lisha fuer die Unterstuetzung bei meinen Klonierungen, Chenlei und Denis fuer das Korrekturlesen. Weiterhin Pascal Rath und Manuel Beltran fuer die Hilfe mit den Analysegeraeten und die lustige Zeit im Fitnessstudio.

Birgit Loeffelhardt, Peter Slaby und Max Koerner fuer den Esprit im Labor und die vielen koestlichen Biere.

Lambrianna Logarnudi, meiner Bachelorstudentin, fuer die Hilfe bei meinem Projekt.

Abschliessend moechte ich noch meiner Familie danken, die mich in jeder Lebenslage unterstuetzt. Meiner Frau Inci und meinen Toechtern Serra-Ida und Sahra-Ela, die sich immer um mich kuemmern. Meinem Bruder Roland, der nicht aufhoert gegen seine Krankheit zu kaempfen, meinem Bruder Klaus, fuer die goettlichen Diskussionen und natuerlich meinen Eltern.

Abstract

A continuously increasing world population, a simultaneously decreasing area of arable land, conflicts and global warming are only a few threats for the global food supply. Deeper knowledge in the plant-microbe interface can help to protect plants against biotic stress, decrease yield loss through adequate safety strategies and is one possible way to feed humanity.

Plants possess a complex system to interact with their environment and to survive in their particular ecological niche. Limited resources need to be distributed between growth, developement and defense. Differentiation between friend and enemy, with a reliable information uptake for a adequate immune reaction, is existential to spare energy. Different sets of extracellular and intracellular receptors thereby sense and process abiotic and biotic signals.

In this work, 83 bacterial strains were screened for immuno-stimulating activity in the model plant *S. pennellii*. The release of ethylene, a defense hormone, was used as stress indicator. Activity-based purification led to the isolation of maculosin, a small molecule produced by many organisms across different kingdoms.

Further investigations about the quantity of maculosin over the fermentation process and the comparison to the initial screen result revealed a difference in the activity. At least two different compounds were present in the analyzed crude culture broth, which both caused ethylene production in *S. pennellii*. One bacterial derived and still concealed substance and the identified maculosin, originated from the peptone medium.

Maculosin is so far unknown to induce ethylene production and callose deposition in *S. pennellii*. Additionally, five derivates of maculosin were tested for ethylene releasing activity. Even cyclo(L-Phe-L-Pro) the closest derivate to maculosin, lacking only a hydroxy group, did not show activity. This result underlines the importance of single functional groups in small molecule signaling.

A compilation of different plants were also tested for stress response due to the treatment of maculosin and its derivates. Except maculosin in *S. pennellii*, no other stress induction could be monitored. This property of *S .pennellii* indicates a specific receptor in this plant. With a forward genetic screen the receptor location of maculosin was narrowed down to a part of chromosome 7.

As additional part of this work, first purification steps were performed to isolate the ethylene-inducing compound out of the culture broth of an *Ensifer* species. Activity-based purification of the supernatant led to two stress causing peptides, one of it with less than 10 kDa in size.

Using the example of maculosin, this work contributes to a better understanding in plant microbe interaction, especially in plant-mediated recognition and response to small signal molecules. It further provides a first purification protocol for two potential *Ensifer* derived elicitors recognized by *S. pennellii* and *S. lycopersicum* M82 respectively.

Contents

List of Figures

List of Tables

List of Abbreviations

ABA . . . . . abscisic acid

AHL . . . . . *N*-acyl homoserine lactone

AIE . . . . . anion exchange chromatography

BAK1 . . . . . BRI1-associated kinase-1

BIK1 . . . . . Botrytis-induced kinase-1

BIL . . . . . backcross introgression line

BKK1 . . . . . BAK1-like 1

BRI1 . . . . . Brassinosteroid insensitive-1

CERK1 . . . . chitin elicitor receptor kinase 1

C . . . . . celsius

CDP . . . . . cyclo dipeptides

Cf . . . . . *Cladosporium fulvum*

CIE . . . . . cation exchange chromatography

cFP . . . . . cyclo(L-Phe-L-Pro)

cGP . . . . . cyclo(L-Gly-L-Pro)

cHP . . . . . cyclo(L-His-L-Pro)

csp . . . . . cold shock protein

cWP . . . . . cyclo(L-Trp-L-Por)

cYP . . . . . cyclo(L-Tyr-L-Pro)

cYW . . . . . cyclo(L-Tyr-L-Trp)

Da . . . . . dalton

DAD . . . . . diode array detector

DAMP . . . . damage associated molecular pattern

EFR . . . . . EF-TU receptor

ET . . . . . ethylene

ETI . . . . . effector triggered immunity

ETS . . . . . effector triggered susceptibility

EtOH . . . . . ethanol

FAO . . . . . Food and Agriculture Organisation

FLS2 . . . . . Flagellin sensing 2

FPLC . . . . . fast protein liquid chromatography

g . . . . . gram

HAMP . . . . herbivore associated molecular pattern

HPLC . . . . . high performance liquid chromatography

h . . . . . hour

HR . . . . . hypersensitive response

IEC . . . . . Ion exchange chromatography

Ig . . . . . immune globulin

IL . . . . . introgression line

ISR . . . . . induced systemic resistance

JA . . . . . jasmonic acid

k . . . . . kilo

KJ . . . . . kilojoule

LC . . . . . liquid chromatography

L . . . . . liter

LRR . . . . . Leucine-rich repeat

MAMP . . . . microbe associated molecular pattern

MAPK . . . . mitogen-activated protein kinase

MeOH . . . . . methanol

MTI . . . . . MAMP-triggered immunity

MS . . . . . mass spetrcometry

MES . . . . . 2-(N-morpholino)ethanesulfonic acid

mA . . . . . milliamps

min . . . . . minute

m . . . . . milli

M . . . . . mol/L

NAMP . . . . nematode associated molecular pattern

n-BuOH . . . . n-butanol

NLP . . . . . necrosis and ethylene-inducing peptide 1-like protein

NLR . . . . . nucleotide binding leucine rich repeat

NMR . . . . . nuclear magnetic resonance

SDS-PAGE . . sodium dodecyl sulfate-polyacrylamide gel electrophoresis

ParAMP . . . parasitic plant associated molecular pattern

PEN . . . . . penicillin extract

PGPR . . . . . Plant-growth promoting rhizobacteria

pmol . . . . . picomol

PTI . . . . . PAMP-triggered immunity

PRR . . . . . pattern recognition receptor

QS . . . . . quorum sensing

RBOHD . . . respiratory burst oxidase homolog

RLCK . . . . . receptor-like cytoplasmic kinase

RLK . . . . . receptor-like kinase

RLP . . . . . receptor-like protein

ROS . . . . . reactive oxygen species

rpm . . . . . rounds per minute

SA . . . . . salicylic acid

SAR . . . . . system acquired resistance

SEM . . . . . scanning electron microscope

SPE . . . . . solid phase extraction

SNP . . . . . single nucleotide polymorphism

SOBIR1 . . . . suppressor of BIR1-1

TF . . . . . transcription factor

TLC . . . . . thin layer chromatography

TRIS . . . . . Tris(hydroxymethyl)aminomethane

1 Introduction

Contents

The overall world population continues to grow. With 7.7 billion people 2019 and a prediction of almost 11 billion people in 80 years. In 2020, already 9.9 % of the global population faced undernourishment, most of them in Asia and Africa [1]. The COVID-19 pandemic, conflicts and extreme weather such as flooding, drought and a rise of temperature caused by climate change are some of the major drivers of food insecurity [2]. Additionally, due to pests a crop failure about 20-40 % yearly is estimated [3].

With a simultaneously growing population crop losses are an even bigger threat,

especially when urbanization and changing climate conditions further restrict arable land areas and promote plant disease spreading [4] [5].

Crop plants are also necessary for other raw materials. In addition to global food supply, they further provide fibers such as cotton and flax, drugs, for example morphine, chemical base products like bioethanol and more. A better understanding of the plant as part of the ecosystem, its structure and the interaction with the environment is a key to successful plant cultivation and with that, the basis for human life. Modern techniques such as gene editing enable us to engineer more resistance crops, higher yields and can further help to speed up plant adaption to new and more extreme environmental conditions [6] [7]. Crop engineering is one efficient opportunity to face upcoming threads of food insecurity, including those of climate change. However, the key is to understand the molecular mechanism underlying the interaction between plant and microbes.

1.1 Plant innate immunity

The earth bears a plethora of different ecosystems. Plants evolved different strategies to thrive in diverse environments. Although different species are unique in development, physiology and secondary metabolites, all higher plants rely on their innate immune system to deal with biotic threats, such as bacteria, viruses, fungi, oomycetes and insects [8] [9].

Besides physiological barriers, such as a cuticule or a rigid cell wall, plants possess an array of pattern recognition receptors (PRRs) located on the plasma membrane. PRRs monitor the apoplastic space in order to detect microbe-associated molecular patterns (MAMPs), conserved molecular structures typical for classes of microbes and not limited to pathogens. PRRs are classified into receptor-like kinases (RLKs) and receptor-like proteins (RLPs) which together can recognize a wide range of molecular patterns. Both classes share an extracellular ligand-binding ectodomain and a transmembrane domain. RLKs have an additional intracellular kinase domain [10] [11]. Extracellular domains vary in their structure and ligand composition,

e.g. leucine-rich repeat (LRR) ectodomains generally sense proteinaceous immunogenic patters. LysM-domain receptors recognize *N*-acetylglucosamine containing ligands like fungal chitin or bacterial peptidoglycan, and the extracellular lectin-domain binds conserved bacterial lipopolysaccharides [12].

Beyond immunity, RLKs are also functionally involved in various developmental processes. The LRR-RLK BRASSINOSTEROID INSENSITIVE-1 (BRI1) for example functions as a receptor for endogenous bassinosteroid hormones to modulate plant growth. Beside its requirement for LRR-RLP function, LRR-RLK SUPPRESSOR OF BIR1-1 (SOBIR1) is a negative regulator of floral organ shedding [13].

Upon ligand perception, RLKs and RLPs need to form a complex with co-receptors of the SERK family e.g. BRI1-ASSOCIATED KINASE-1 (BAK1) or SOBIR1 to transfer the received signal into the cell [14]. One of the best studied examples is the recognition of flg22, one active epitope of bacterial flagellin, by the FLAGELLIN SENSING 2 (FLS2) receptor. The presence of flg22 releases the BAK1 negative regulators BAK1-INTERACTING RLK-2/3 (BIR2 and BIR3), which leads to a FLS2-BAK1 heterodimerization followed by BOTRYTIS-INDUCED KINASE-1 (BIK1) activation. BIK1 dissociates from the FLS2-BAK1 complex and phosphorylates RBOHD to initiate ROS production. In addition, BIK1 associates with other RLCK VII members and activates the mitogen-activated protein kinase (MAPK) cascade and further downstream signaling [12].

This process is also referred to as pattern triggered immunity (PTI) and includes beside ROS release and MAPK activation manifold defense reactions, e.g. stomata closure, defense hormone activation, callose deposition and the secretion of secondary metabolites and hydrolytic enzymes [15]. Since the active elicitor epitope flg22 is embedded in the flagellin polymer, the secretion of hydrolases actively unleash the immunogenic compound and further promotes PTI defense [16].

PTI is considered as sufficient to ward of non-adapted microbes and causes broad spectrum resistance [12]. However, adapted pathogens are able to undermine this defense mechanism, either by interfering with the recognition at the plasma membrane level or by suppressing PTI through effectors. Effectors are usually

small proteins secreted from pathogens into the cell apoplastic space or cytoplasm of the host, via penetration of the cell wall with haustoria (fungi, oomycetes and parasitic plants) or the type III secretion system (bacteria) causing effector triggered susceptibility (ETS) [17].

Various targets in the PTI downstream signaling are described. E.g. AvrB and AvrRpm, effectors of *Pseudomonas syringae*, target the early signaling process through RIN4 (RPM1-interacting protein4) phosphorylation. RIN4 is located on the plasma membrane and negatively regulates PTI. This leads to an enhanced RIN4 activity and a decreased PTI activation [18]. The effector XopD from *Xanthomonas campestris* represses the *Arabidopsis thaliana* (hereafter referred as *Arabidopsis*) transcription factor AtMYB30, which is located in the cell nucleus and acts as positive regulator of cell death associated response. This results in suppression of hypersensitive response (HR) and plant defense [19].

Plants in turn respond to the threat with intracellular nucleotide binding leucine rich repeats (NLRs) which directly or indirectly detect the presence of effectors and induce effector triggered immunity (ETI), a strong defense reaction, which often leads to a HR and programmed cell death. The observation of no direct binding between nucleotide-binding domain leucine-rich repeats (NB-LRRs) and Avr proteins in many cases led to the "guard hypothesis", which suggests NB-LRRs are negatively regulated by their guardees. Effector binding then results in the activation of a resistance (R) protein and ETI induction [20]. Indirect recognition is known for example from the *Arabidopsis* NLR RPM1, which guards RIN4 and triggers ETI after recognition of the effectors AvrB and AvrRpm1 [18]. However, also direct effector recognition was found from the downy mildew pathogen *Hyaloperonospora arabidopsidis* effector ATR1, which is detected by the TNL RPP1 from *Arabidopsis* [21].

The concept that disease resistance in plants requires two complementary genes, an avirulence (Avr) gene in the pathogen and a matching R gene in the host is

called the 'gene for gene hypothesis'. Plants activate defense mechanisms upon R-protein-mediated recognition of pathogen-derived Avr products [22]. This suggests effectors and ETI as more species specific [17].

1.1.1 PTI and ETI - a two-branched immune system

Since years plant innate immunity has been described as two layers of defense, including PTI and ETI. While PRRs located on the plasma membrane caused PTI upon MAMP perception and broad-spectrum resistance. ETI was triggered species specific and inside the cell by intracellular immune receptors, such as NLRs.

To illustrate the evolutionary relationship between PTI and ETI, a so called zig-zag model was proposed. This model contains 4 phases: Phase 1, MAMPS are recognized by PRRs resulting in PTI. Phase 2, successful pathogens deploy effectors, suppress PTI and cause ETS. Phase 3, effectors are recognized by NB-LRRs and trigger ETI. Phase 4, natural selection drives pathogens to new effectors and plants to new NB-LRRs [23]. However, this model is based on the assumption of a clear difference between PTI and ETI.

Nevertheless, the model of two independent branches of immunity has its limitations. For example, it does not explain the finding, that also the cell-surface receptors Cf-2, Cf-4, Cf-5 and Cf-9 in *Solanum lycopersicum* sense effectors, secreted by the leaf mold pathogen *Cladosporium fulvum* [24]. Furthermore, also some effectors are known to be conserved, e.g. the LysM effector Ecp6, secreted by *C. fulvum*, which suppresses chitin-triggered immunity. This effector is conserved in the *C. fulvum* family with orthologs across the fungal kingdom [25] [26]. The two-branched innate immune system with its classification of MAMPs or effectors based on their mode of action or their occurrence is therefore inaccurate [27].

To overcome classification issues, different definitions of immunogenic patterns have been suggested. For example Vleeshouwers and Oliver [28] defined elicitors, host-specific toxins and effectors as effectors including every immunostimulating substance: '... effectors as pathogen-produced molecules that have a specific effect on one or more genotypes of a host or non-host plant.' However, a new

definition can not explain other issues, namely the question whether there is a clear border between the two branches PTI and ETI [27] [29] [30]. The overlap between PTI and ETI immune responses in cell wall fortification through callose and lignin or the production of antimicrobial secondary metabolites are only two examples for this doubt [31]. Beside that, lately findings exhibited a connection between both defense mechanisms.

1.1.2 Two branches connected

PTI and ETI are activated in different compartments, involve different early signaling cascades but rely on similar sets of genes. Recent studies show that intracellular receptors primarily potentiate the signal of PTI. HR for instance, requires NLR signaling, but is reinforced by the activation of PRRs [32]. Furthermore, the ROS production by the NADPH oxidase RBOHD is proposed as connection between PRR- and NLR- mediated immunity [33].

Pruitt et al. [34] published that the EDS1-PAD4-ADR1 node, located on the inner side of the plasma membrane, is essential for for PTI and ETI immunity. They further hypothesize that cell surface LRR-RLPs and NLRs share a genomic organization into gene clusters. Both receptor types further have a large sequence diversity which could be evolved by similar evolutionary dynamics. All those data point to a new understanding of plant innate immunity.

However, due to its complexity, the plant has to be understood as a whole organism with a limited amount of resources and a permanent balance between development, growth and defense [35]. Many autoimmune mutants are reported in *Arabidopsis*, caused by the up regulation of NB-LRR Proteins and are often linked with dwarfism and spontaneous cell death [36] [37]. Additionally, a single gene can influence the plant development as well as the regulation of immunity. The ERECTA (ER) gene for example, controls plant growth and beside that, is a regulator for resistance to *Plectosphaerella cucumerina* in *Arabidopsis* [38] [29].

1.1.3 Perception and action, the Danger model

A recently proposed model, which is referred to the metazoans, overcomes the limitations of the PTI/ETI framework. This model categorized every pattern leading to a immune response as danger signals and is therefore called 'Danger model' [29] [30] [39].

Danger signals can be divided into three different groups; exogenous (non-self), endogenous (self) and abiotic stressors. The latter one has been described, but is not established so far. Exogenous signals contain all patterns fom microbes (MAMPs), herbivores (HAMPs), nematodes (NAMPs) and parasitic plants (ParAMPs) as well as recognized effectors. Endogenous signals can be further divided into primary endogenous danger signals, which consist of all kinds of DAMPs, and secondary endogenous danger signals or immunity modifiers. Immunity modifiers include plant endogenous peptides which are secreted actively and shape the immune responses upon infection, such as systemin in tomato [40] and the plant elicitor peptides (Pep) found in *Arabidopsis* and later in maize [41] [42]. Based on the analogy in metazoans, these immune shaping molecules should be termed phytocytokines [30].

This model also suggests that the presence of an elicitor is not sufficient for a strong immune response and therefore follows the new paradigm. It proposes additional signals released during the infection process as required for proper defense [43]. This model also provides a plausible explanation to the fact, that a plant with a bacterial microbiome does not show any symptoms of permanent stress [30] [34].

1.2 Phytohormone regulation in plant defense

Phytohormones are small signal molecules which act in low concentrations. They are essential for the regulation of plant growth, development, reproduction and defense. Typical phytohormones are ethylene (ET), jasmonic acid (JA), salicylic acid (SA), auxines, cytokinins, abscisic acid (ABA), gibberellins and brassinosteroids [31]. All phytohormones have multiple functions in physiological and developmental processes. E.g. ET mediates seedling emergence, leaf and flower senescence, fruit

ripening and organ abscission. However, ET together with JA and SA is also known for its functions in plant immunity [44]. Those hormones act in antagonistic or synergistic manner and arbitrate a wide range of adaptive plant responses. Defense reactions can be divided into local and systemic [31].

1.2.1 Local defense

Apart from abiotic stress caused through high radiation, high salt concentration, drought or stagnant moisture, Et, JA and SA are key players for a proper response to biotic stress like pathogenic infections. Pathogens can be divided into biotrophs (derive nutrients from living cells) such as *C. fulvum* and *Blumeria graminis*, necrotrophs (derive nutrients from dead cells) like the fungi *Botrytis cinerea* and *Leptosphaeria maculans*, and hemibiotrophs (derive nutrients from living cells during an initial state of infection and kill the host cell in a later stage) such as the fungus *Ustilago maydis* and the oomycete *Phytophthora infestans* [28]. An appropriate quantity and composition of ET, JA and SA, together with the timing eventually determines the nature and effectiveness of the response and varies on one hand among plant species and on the other on the lifestyle and infection strategy of the invader [45]. Upon biotrophic attack, the plants respond with a strong SA response, HR and cell death. This strategy however would fuel necrotrophic attackers [46]. Necrotrophs therefore have to be distracted by a different set of defense responses, which are initiated through an ET and JA mediated signaling pathway. SA has therefore an antagonistic effect on JA, whereas ET acts with JA mostly in a synergistic manner [31]. In parallel to necrotrophs, the wound response which is triggered against insect herbivores is regulated by a JA dependent pathway [47] [48].

1.2.2 Systemic defense

Systemic resistance is besides the direct defense mechanisms a plant reaction to biotic stress conditions. This process occurs in order to prime distant cells against pathogenic invaders. Two different forms are described.

Systemic aquired resistens

Upon pathogenic attack, the plant triggers so called systemic acquired resistance (SAR), a long lasting and broad spectrum defense mechanism. An induction of SAR occurs locally, at the side of infection and systemically in distant plant tissue and involves increased levels of SA. A specific set of pathogenesis-related protein (PR) genes gets activated, which encodes proteins with antimicrobial activity [49] [50].

Induced systemic resistance

Beneficial soil-borne microorganisms like mycorrhizal fungi and plant growth-promoting rhizobacteria induce a state of induced systemic resistance (ISR). In this case, the plant is stimulated for enhanced defense, although PR genes itself are not activated. ISR is regulated by JA and ET [51].

1.2.3 Phytohormones produced by microorganisms

The complex interplay between the phytohormones enables the plant to react to biotic stressors in a adequate mode. However, also some non-pathogenic bacteria as well as host adapted pathogens are able to influence the hormone signaling by the plant. While *Pseudomonas putida* promotes root growth with the release of auxin, the Crown Gall disease-causing pathogen *Agrobacterium tumefaciens* as well as *Agrobacterium rhizogenes*, *Pseudomonas savastanoi* and *Pantoea agglomerans* use IAA for uncontrolled cell proliferation and promotion of virulence [52].

1.3 Phytotoxins

Especially plant pathogens with a necrotrophic or hemibiotrophic lifestyle are known to produce and secrete phytotoxins as strategy to conquer and finally kill the host plant [53]. Phytotoxins cover a wide group of substances, from small molecules like sclerin, produced by the fungus *Sclerotinia sclerotiorum* [54] to proteins, for instance NEP1-like proteins (NLPs), which were first found in the culture broth of *Fusarium oxysporum* [55] [56]. Defense responses to toxins are similar to those activated

by effectors including ET biosynthesis, ROS accumulation, callose deposition, extracellular alkalinization and phytoalexin synthesis, since the pathways of the defense hormones ET, JA and SA are overlapping and affecting each other [57].

1.3.1 Mode of action - targets of toxins

A number of cellular targets are known for their interaction with phytotoxins, showing versatile ways to overcome the plant cell [58]. The AAL-toxin for example undermines membrane integrity through inhibition of sphingolipids biosynthesis in leaves [59]. Photosensitizers like cercosporin, elsinochrome A and rubbellin D absorb light energy and generate ROS to damage the plant cell [60]. Tentoxin, produced by *Alternaria* species targets the ATP-hydrolysis in chloroplasts, which causes an energy breakdown inside the cell [61]. *Ustilago maydis* causes tumor induction through the production of high concentrations of the signal molecule auxin [62]. Victorin, produced by the fungus *Cochliobolus victoriae* inhibits mitochondrial photorespiration [63].

Recognition of phytotoxins occurs either indirect through disruption of the cell integrity and DAMP release or direct through NB-LRR receptor proteins. Interestingly, NB-LRR receptor proteins itself, known for their function in disease resistance, can act as target of virulence factors and cause susceptibility. Oat plants containing the R gene Pc-2 show resistance against the rust fungus *Puccinia coronata*. The same gene induces susceptibility to the pathogen *Cochliobolus victoriae*. Victorin thereby induces resistance-like physiological changes, e.g. callose deposition, ethylene accumulation, ROS burst and others [57].

However, similar to effectors, not all toxins activate defense responses. Deoxynivalenol (DON) for instance, a family member of trichothecenes is produced by necrotrophic *Fusarium* species, acts as translational inhibitor in ribosomes without induction of defense [64]. In some cases, i.e. the host-specific phytotoxin maculosin, produced by *Alternaria alternata*, a detailed mechanism remains unclear.

1.3.2 Toxins as natural herbicides

Phytotoxins exhibit various biological activities against plants and weeds. This makes them to a potential source of biological herbicides.

Many microbe-derived herbicides have been found during the last years, but only few fulfill the requirements for a widespread use [65]. Maculosin for instance has been found in the fungus *A. alternata* among other microbes [66] [67]. This simple cyclic dipeptide composed of L-trypthophan and L-prolin has been considered as specific herbicide against spotted knapweed, an invasive plant in the United States [68]. However, the substance was not as effective as expected in the beginning. Another example is the recently found 7-deoxy-sedoheptulose (7dSh) produced by *Synechococcus elongatus*. This sugar acts as inhibitor of the dehydroquinate synthase as part of the shikimate pathway and is discussed as a potential alternative to the controversial use of glyphosate [69].

1.4 Aims of the thesis

In this study we investigate the recognition of 83 non-pathogenic soil bacteria in the tomato lines *Solanum pennellii* and *Solanum lycopersicum* M82, in order to find and purify a novel ethylene-eliciting substance. The defense hormone ethylene is used as stress indicating output. This study further explores activity relevant structural motifs of the purified molecule and localizes gene targets involved in the perception process via a forward genetic screen.

2

Materials and Methods

Contents

2.1 Materials

2.1.1 Bulk chemicals

- Water (HPLC grade), methanol (HPLC grade), ethanol (HPLC grade), n-butanol (HPLC grade), dichlormethan (HPLC grade), ammonium sulfate (99 %, crystalline). The chemicals were purchased from Carl Roth.

2.1.2 Other chemicals

- Luminol mastermix (1 mL): 986 µL H_2O, 10 µL Luminol L-012 20 mM, 4 µL peroxidase (5 mg/mL).
- Rotiphorses Gel 30 (Carl Roth, Karlsruhe): 30 % acryl amide solution

2.1.3 Media

All Media were used after autoclaving, with a pH 7.3. For plates, 15 g/L agar was added.

- Tryptic soy broth (TSB) ready to use powder: 23 g/L.
- Super optimal broth (SOB): 20 g/L Bacto tryptone, 5 g/L yeast extract, 0.5 g/L NaCl, 0.16 g/L KCl, 10 mL/L $MgCl_2$ (1 M), 10 mL/L $MgSO_4$ (1 M).
- Peptone medium: 17 g/L casein peptone, 2.5 g/L glucose, 2.5 g/L NaCl, 2.5 g/L K_2HPO_4.
- Minimal medium: 2.5 g/L NaCl, 2.5 g/L K_2HPO_4, 2.5 g/L glucose, 2.5 g/L $(NH_4)_2SO_4$.

2.2 Organisms

2.2.1 Bacteria

20 µL Bacterial suspension (glycerol stock) was grown on a agar plate. After two days one colony of each strain was added to 3 mL of liquid culture, containing the same growth medium. After incubation (28 °C, 200 rpm), the preparatory culture was added into 2 L flasks with 500 mL of sterile growth medium. The grown Bacteria were harvested after 3 days.

Cells were separated from the supernatant via centrifugation (5000- 18000 rpm, 20 min). The cell pellet was resuspended in 2-(N-morpholino)ethanesulfonic acid (MES) buffer (30 mM, pH 5.7) and solubilized with a sonicater (65 % amplitude, 3 s pulse frequency until 2 KJ). The decomposed cell residues were removed.

2.2.2 Plants

Solanum lycopersicum cv. M82, _Solanum pennellii_ and the introgression line mapping population

All used tomato plants were grown in a greenhouse (16 h light, 22°C and 30- 40 % humidity), on Arabidopsis-soil. Leafs of the plants were used after 4- 5 weeks.

Table 2.1: Insertion lines of the mapping population*

Chromosome	Insertion lines
1	1-1, 1-3, 1-4
2	2-1, 2-2, 2-4, 2-5, 2-6
3	3-1, 3-3, 3-4, 3-5
4	4-1, 4-2, 4-3, 4-4
5	5-1, 5-2, 5-3, 5-4, 5-5
6	6-2, 6-4
7	7-1, 7-2, 7-3, 7-4, 7-5, 7-5-5
8	8-1, 8-2, 8-3
9	9-1, 9-2, 9-3
10	10-1, 10-2, 10-3
11	11-1, 11-2, 11-3, 11-4
12	12-1, 12-2, 12-3, 12-4

*The material was developed by and/or obtained from the UC Davis/C.M. Rick Tomato Genetics Resource Center and maintained by the Department of Plant Sciences, University of California, Davis, CA 95616.

Arabidopsis thaliana

The *A. thaliana* ecotype Col-0 (ICE73) plants were grown in a growth chamber (8 h light, 22 °C and 40- 60 % humidity) on GS90-soil containing gnatrol. Leafs of the plants were used after 5 weeks.

Other plants

The following plants were grown in a growth chamber (8 h light, 22 °C and 40 - 60 % humidity) on potting soil: *Lotus japonicus*, *Brassica napus*, *Brassica oleracea*, *Solanum tuberosum* (Désiréé), *Centaurea stoebe*, *Centaurea cyanus*, *Capsicum*

annuum, *Helianthus annuus*, *Lactuca*, *Marian thistle*, *Solanum lycopersicum* (Aunt Ginnys Purple Tomato). The leafs of the plants were used after 5 weeks.

Soil types

Arabidopsis-soil: 70 L CL Topf (Patzer Erden, Sinntal-Altengronau) and 8 L sand (Flammer Bauunternehmung GmbH & Co. KG, Tübingen) were mixed and sieved (8 x 10 mm).

GS90-soil: 70 L CL Topf grob 1+1 (Patzer Erden, Sinntal-Altengronau) and 10 L Palabora-vermiculite (Isola Vermiculite GmbH, Sprockhövel) were mixed, sieved (8 x 10 mm) and steamed.

2.3 Methods

2.3.1 Biochemical Methods

Ion exchange chromatograhpy (IEC)

An Aekta pure fast protein liquid chromatography (FPLC) system (Cytiva) was used for ion exchange chromatography (IEC). Buffers were prepared according to the manufactureres protocol.

AIE: The strong anion exchange chromatography column, HiTrap Q Fast Flow 5 mL column (Cytiva) was used with TRIS-HCl (20 mM, pH 8.5) as buffer A and TRIS-HCl (20 mM, pH 8.5) + NaCl (1 M) as elution buffer B. The column was washed with 25 mL buffer A (5 mL/min) and 200 mL sample (pH 8.5) was loaded to the column (5 mL/min). After washing the column with 25 mL buffer A, a three steps gradient was used (30 %, 60 % and 100 % buffer B, 5 mL/min) for elution. All fractions were collected.

CIE: The strong cation exchange chromatography column, HiTrap SP Fast Flow 5 mL column (Cytiva) was used with MES (50 mM, pH 5.5) as buffer A and MES (50 mM, pH 5.5) + NaCl (1 M) as elution buffer B. The column was washed with 25 mL buffer A (5 mL/min). 200 mL sample was adjusted to pH 5.5 and loaded to the column (5 mL/min). After washing the column with 25 mL buffer

A, a three steps gradient was used (30 %, 60 % and 100 % buffer B, 5 mL/min) for elution. All fractions were collected.

Size exclusion chromatography (SEC)

3 mL of sample (450 mg/mL) were applied on a 73 cm sephadex LH-20 agarose gel packed column. MeOH was used for elution (1 mL/min). Fractions were collected over night in 15 min intervals with a automated fraction collector.

High performance liquid chromatography (HPLC)

A HPLC System (Agilent Technologies Deutschland GmbH, Waldbronn) was used with a semi preparative reverse phase C18 column (particle size 5 µm, 10 mm diameter, Dr. Maisch) for liquid chromatography, with methanol (HPLC grade) as buffer A and water (HPLC grade) as elution buffer B. 50 µL (1 mg/mL) sample was applied via injection loop. Absorption was monitored with a DAD-detector (DAD-3000RS). Fractions were collected via a fraction collector (Ultimate AFC-3000).

SDS-page

The sodium dodecyl sulfate-polyacryl amide gel electrophoresis for proteins from 10 - 100 kDa was performed like described in LAEMMLI [70] and Sambrook [71]. 15 % separating gels and 5 % stacking gels were applied in a BioRad chamber system (25 mA, 1 h). 5 µL of a prestained PageRuler protein ladder mix (Thermo Fisher Scientific, Karlsruhe) was used as size marker.

Mass spectrometry compatible silver stain

The performed SDS page was fixed (1 h) in a mixture of 50 % MeOH, 12 % CH_3COOH, 0.5 mL/L HCOH and H_2O, followed by washing (3 x 20 min) with 50 % EtOH. The gel was pretreated (~1 min) with 0.2 g/L of $Na_2S_2O_3$ x 5 H_2O. After washing with H_2O, impregnation was carried out (1 h) using a solution of 2 g/L $AgNO_3$, 0.75 mL/L 37 % HCOH. The washing step, with distilled water, was repeated. The gel was developed (~5 min) with a solution of 60 g/L Na_2CO_3, 0.5 mL/L 37 % HCOH and 4 mg/L $Na_2S_2O_3$. After rinsing the gel with distilled water,

the reaction was stopped with a solution of 50 % MeOH and 12 % CH_3COOH. All reagents were prepared freshly.

Enzymatic digest

50 µL sample + 5 µL of Pronase E enzyme mix (VWR, Bruchsal) were mixed in a 1.5 mL micro reaction tube (Eppendorf, Wesseling) and incubated at 37 °C over night.

Dialysis

Dialysis was performed with a 1 kDa cut-off membrane tube (Thermo Fischer Scientific, Karlsruhe). Preparation of the membrane was done according to the manufactureres protocol. After loading the sample into the membrane, both sides were capped with fasteners. The membrane was placed in a beaker containing 10 times the buffer volume. Equilibration was set at 6 °C over night, stirring with 20 rpm.

Protein precipitation

Ammonium sulfate crystalline (Carl Roth, Karlsruhe) was added to 2 L of culture broth (~4 M). The precipitated protein was separated (5000 rpm, 5 min) and resolved in MES buffer (30 mM, pH 5.7).

Amberlite XAD16 resin extraction

100 g Amberlite XAD16 resin (Thermo Fischer Scientific, Karlsruhe) was activated according to the manufacturers protocol and packed into a column. 1 L of sample was filtered through the column (3 mL/min). The resin was washed with 3 L of distilled water. After elution with 200 mL MeOH, the solvent was removed via rotary evaporator. A concentration of 450 mg/mL was set with MeOH as solvent.

Solid - liquid extraction

10 g of lyophilized supernatant were weight into a 50 mL Falcon tube. Extraction was done with 3 x 30 mL solvent while rotating for 30 min at room temperature. After removing the remaining solid, unified extracts were dried and resolved in MES buffer (30 mM, pH 5.7).

2.3.2 Bioassays

Ethylene assay

Leafs of five weeks old plants were cut into rectangles of 0.5 x 0.7 cm and stored in distilled water over night. Three leaf pieces were put into a test tube containing 400 µL of MES buffer (30 mM, pH 5.7). After adding the sample, the tube was sealed with a rubber septum. Incubation took 3-4 hours on a shaker, with a rate of 125 rpm. One mL of air was injected to a gas-phase chromatograph (Shimazu, Reinach). The concentration of ethylene was measured in ppm.

Reactive oxygen species assay

Leafs of five week old plants were cut into squares of 0.5 x 0.5 cm and stored in distilled water over night. One leaf piece was added into every well of a 96 well plate, containing 90 µL of a luminol master mix. After 30 min of equilibration in the dark, 10 µL of the samples was added and the ROS production was measured via a Mithras LB 940 luminometer (Berthold Technologies, Bad Wildbad) in 1 min intervals.

Callose deposition assay

The method was adopted and modified from [72]. The leafs of *S. pennellii* plants were infiltrated with different concentrations of a maculosin dilution. PEN (5 mg/mL) was used as a positiv control. After 72 h infiltrated tissue was removed using a cork borer and bleached with 95 % EtOH. Bleaching took place in an incubator at 37 °C until no chlorophyll was left. The leaf disks then were washed with 70 % EtOH and distilled water. Staining was performed using a solution of 0.2 % Anilin blue in 150 mM K_2HPO_4, pH 9.5. and incubated over night at 8 °C, protected from light. The stained leaf disks were placed on glass slides, mounted with 50 % Glycerol and covered with a cover glass. Fluorescence was determined by a AXIO ZOOM V.16 microscope (Zeiss, Jena) with an UV-DAPI filter.

2.4 Data bases and software

BLAST data base, Solgenomics.net, R, R Studio and R Markdown (Thesis Template for R Markdown [73]), Unicorn control software (FPLC), Chromeleon control software (HPLC)

3 Results

Contents

3.1 Screen for ethylene-inducing substances in a collection of rhizosphere bacteria

A collection of 83 bacterial strains, isolated from the rizhosphere of a field grown *Arabidopsis thaliana*, was tested for immunostimulating substances in the tomatoe ecotypes *Solanum pennellii* and *Solanum lycopersicum* cv. M82, hereafter called M82. The collection was provided by Paul Schulze-Lefert (MPI, Köln). The sequences of all strains are available in the BLAST data base [74]. For the two tomato lines Eshed and Zamir [75] created a mapping population, which includes 50 introgression lines with a M82 background and *S. pennellii* insertions distributed on all 12 chromosomes. The sequence of every line is available on solgenomics.net. Those tools allow to trace back a trait difference between *S. pennellii* and M82 to its location on the chromosome and further qualify trait related genes.

Ethylene production served as output and indicator for a present receptor-ligand pair. Samples which revealed ethylene activating properties were retested. Untreated culture broth was used as control. Ethylene concentrations two times higher than the control or with minimum 1 pmol ethylene/ml air were evaluated as active. An overview of the activity screen is provided in table 3.1. Additionally, all strains were explored for flagella by comparing the protein sequence of flg22 (QRLSTGSRINSAKDDAAGLQIA [76]) with the respective strain sequence in the BLAST data base.

Table 3.1: Overview of the tested rizosphere bacteria, their immunostimulant property and the flg22 sequence comparison

Stock ID	Strain ID	Genus	Flagellin*	*S. pennellii*	M82
1A1	Root9	*Pseudomonas*	✓[1]	x[2]	x
1A2	Root73	*Rhizobium*	x	x	x
1A4	Root172	*Mesorhizobium*	✓	x	x
1A6	Root329	*Pseudomonas*	x	x	x
1A8	Root480	*Rhodanobacter*	✓	x	x
1A9	unknown	unknown	-[3]	-	-
1A10	Root627	*Rhodanobacter*	✓	x	x
1A11	Root670	*Bosea*	✓	x	x
1B2	Root74	*Ensifer*	x	x	x
1B3	Root127	*Ensifer*	x	x	x
1B4	Root179	*Rhodanobacter*	x	s[4], bs[5]	x
1B5	Root258	*Ensifer*	x	s	x
1B8	Root562	*Pseudomonas*	✓	s, bs, c[6]	x
1B9	Root482	*Rhizobium*	x	x	x
1B10	Root630	*Pseudoxanthomonas*	✓	s	bc[7]
1B12	Root916	*Lysobacter*	x	x	x
1C1	Root31	*Ensifer*	x	x	x
1C2	Root76	*Lysobacter*	x	s, bs	x
1C3	Root133	*Massilia*	✓	x	x
1C5	Root267	*Acidovorax*	✓	x	x
1C6	Root342	*Caulobacter*	✓	x	x
1C7	Root411	*Variovorax*	x	x	x
1C8	Root491	*Rhizobium*	✓	x	x
1C9	Root564	*Rhizobium*	✓	x	x
1C11	Root685	*Devosia*	x	x	x
1C12	Root919	*Cupriavidus*	-	-	-
1D1	Root50	*Sphingomonas*	✓	x	x
1D2	Root77	*Phenylobacterium*	✓	x	x
1D3	Root142	*Ensifer*	x	x	x
1D5	Root268	*Rhizobium*	x	x	x
1D9	Root565	*Achromobacter*	✓	x	x
1D10	Root651	*Rhizobium*	x	s	s
1D11	Root690	*Lysobacter*	x	x	x
1D12	Root954	*Ensifer*	x	x	s
1E1	Root65	*Pseudoxanthomonas*	✓	x	x
1E2	Root83	*Bordetella*	✓	s, bs, bc	x
1E3	Root149	*Rhizobium*	✓	s	s
1E5	Root274	*Rhizobium*	x	x	x
1E7	Root423	*Ensifer*	x	x	x
1E8	Root552	*Mesorhizobium*	✓	s, bs	x
1E9	Root568	*Acidovorax*	✓	s, bs, c, bc	x

Stock ID	Strain ID	Genus	Flagellin*	*S. pennellii*	M82
1E12	Root983	*Lysobakter*	x	s	x
1F1	Root68	*Pseudomonas*	✓	x	x
1F2	Root96	*Lysobakter*	x	x	x
1F3	Root154	*Sphingopyxis*	✓	x	x
1F4	Root214	*Sphingopyxis*	✓	x	x
1F5	Root275	*Acidovorax*	✓	x	x
1F6	Root381	*Bosea*	✓	x	x
1F7	Root434	*Variovorax*	x	x	x
1F8	Root554	*Mesorhizobium*	✓	x	x
1F9	Root569	*Pseudomonas*	✓	x	bc
1F10	Root656	*Caulobacter*	✓	x	x
1F11	Root700	*Phenylobacterium*	✓	x	x
1F12	Root1203	*Rhizobium*	✓	x	x
1G1	Root70	*Acidovorax*	✓	x	x
1G2	Root100	*Aminobacter*	✓	x	x
1G3	Root157	*Mesorhizobium*	✓	x	x
1G4	Root219	*Acidovorax*	✓	x	x
1G5	Root278	*Ensifer*	x	x	x
1G6	Root401	*Pseudomonas*	✓	x	x
1G8	Root558	*Ensifer*	x	x	x
1G9	Root604	*Lysobacter*	x	x	x
1G10	unknwon	unknown	-	-	-
1G11	Root708	*Rhizobium*	✓	x	x
1H1	Root71	*Pseudomonas*	✓	x	x
1H3	Root170	*Bordetella*	x	x	x
1H4	Root231	*Ensifer*	x	x	x
1H6	Root402	*Acidovorax*	✓	x	x
1H7	Root473	*Variovorax*	✓	x	x
1H8	Root559	*Lysobacter*	x	x	x
1H10	Root667	*Lysobacter*	x	s, bs	x
2A2	Root1277	*Phenylobacterium*	✓	x	x
2A3	Root1334	*Rhizobium*	x	x	x
2A5	Root318D1	*Variovorax*	x	s	x
2B2	Root1279	*Brevundimonas*	✓	x	x
2B4	Root1485	*Massilia*	✓	x	x
2C1	Root1221	*Rhizobacter*	✓	x	x
2C2	Root1280	*Acinetobacter*	x	bs	x
2C4	Root1497	*Sphingopyxis*	✓	x	x
2E2	Root1290	*Phenylbacterium*	✓	s, bs	bs
2F2	Root1294	*Sphingomonas*	✓	x	x
2G1	Root1252	*Ensifer*	x	s	x
2G2	Root1298	*Ensifer*	x	s	x
2G4	Root198D2	*Duganella*	✓	x	x
2G5	Root483D2	*Rhizobium*	✓	s, bs	x

Stock ID	**Strain ID**	**Genus**	**Flagellin***	***S. pennellii***	**M82**
2H2	Root1312	*Ensifer*	x	x	x

*based on the comparison with the BLAST data base (sequence: QRLSTGSRINSAKDDAAGLQIA [76]).

[1]yes

[2]no

[3]unknown

[4]supernatant

[5]boiled supernatant

[6]cell extract

[7]boiled cell extract

The strains were grown and processed as described in the method section. After three days of growth, the culture was harvested and cells and supernatant were separated via centrifuge. The cell pellet was resuspended in MES buffer and disrupted with a sonicater. Remaining cell residues were removed. With this, every strain provided two samples, the supernatant and the cell extract, in total 166 samples, which were tested for ethylene inducing activity in the described tomato lines *S. pennellii* and M82. Since boiling can either destroy the activity of a sample, e.g. by destroying a necessary folding structure of a protein, or improve the accessibility of a poor soluble compound, all samples were also tested after heat treatment (95 °C, 10 min). Beside the presence and functionality of elicitors, other factors e.g. additional secreted effectors can influence the ethylene response.

In total: 63 strains did not lead to a significant ethylene response. 4 strains (1B10, 1D10, 1E3 and 2E2) showed activity in both tomato ecotypes. 2 strains (1D12 and 1F9) caused ethylene accumulation only in M82 and 14 strains (1B4, 1B5, 1B8, 1C2, 1E2, 1E8, 1E9, 1E12, 1H10, 2A5, 2C2, 2G1, 2G2 and 2G5) only in *S. pennellii*.

Due to several reasons, a decision for further purification was done in favor of the culture supernatants of the two strains *Rhodanobacter* (1B4) and *Ensifer* (2G2).

First, the significantly high ethylene responses of both samples appeared to be dose dependent (Fig. 3.1 and Fig. 3.29). Furthermore, the activity of both strains increased in an initial stage of fermentation and decreased in a later stage (Fig. 3.7). This time dependence suggests a substance produced by the strain. Second, the sequence comparison of flg22 with the genome of both strains via the BLAST data base indicated an elicitor different from flagellin, because both strains lack flagellin. For the tomato system, two active epitopes of flagellin are known, namely flg22, recognized by the FLS2 receptor and flgII-28, perceived by the receptor FLS3 [77]. Since flagella are widespread within the bacterial kingdom, an exclusion of this plant immunoactive protein in the strain of interest is indispensable. Even as contamination, the presence of trace amounts of flg22 is sufficient to disturb an activity based screen or purification [78]. Third, because the immuno-reactions seem to be different in both tomato ecotypes *S. pennellii* and M82 (Fig. 3.1 and Fig. 3.29), the requirement for the use of the mapping population to find a corresponding receptor was fulfilled. Finally, with the focus on *S. pennellii*, all known bacterial derived elicitors for the tomato system can be excluded. Beside the two active epitopes of flagellin, only the structurally conserved cold shock protein (csp) with its active epitope csp22 is known to cause ethylene accumulation in tomato. Csp22 activates the tomato receptor kinase cold shock protein receptor (CORE). Interestingly, CORE was identified with the same tomato mapping population as used in this work [79]. The required phenotypic difference between *S. pennellii* and M82 was fulfilled, due to the fact that csp22 is only active in M82 and not in *S. pennellii*. Conversely, the focus on bacterial strains which showed ethylene producing activity only in *S. pennellii* already exclude the possibility of csp22 as elicitor.

Taken together this finding suggests a secreted elicitor from *Rhodanobacer* (1B4) as well as form *Ensifer* (2G2) which can be recognized by *S. pennellii* but not by M82 and which are different from the already known bacterial derived elicitors.

3.2 Activity based purification of the *Rhodanobacter* (1B4) supernatant

3.2.1 Characterisation of the supernatant activity

A dose dependent ethylene production assay was performed with the *Rhodanobacter* supernatant as well as the cell extract (Fig. 3.1 and Fig. 3.2). The supernatant was compared to the equal volume of untreated peptone medium as control. Also higher volumes of medium did not induce a significant ethylene production.

The fold change was calculated with the equation: fold change = supernatant/medium and indicates the factor of the activity/background ratio, Fig. 3.1 B and D. With increased volumes of supernatant a higher ethylene accumulation in *S. pennellii* is visible, which suggests the active compound as bacterial-derived. Compared to the medium, the M82 tomato does not react to the *Rhodanobacter* supernatant in a dose dependent manner. A clear difference between both tomato lines is exhibited.

A dose dependent ethylene bioassay was also performed for the *Rhodanobacter* cell extract, Fig. 3.2 A.

Compared to supernatant and medium, the cell extract does not trigger a significant amount of ethylene. This finding suggests that a secreted molecule is recognized by the tomato line *S.pennellii*. To explore, whether the active molecule is heat sensitive, 1 mL of supernatant was boiled for 10 min at 95 °C and tested in an ethylene assay, Fig. 3.2 B. Two different volumes were tested, 20 µL and 50 µL. Medium treated the same way was used as control. Although the total response with nearly 0.9 pmol/mL air of 50 µL supernatant is not very high, the comparisons before and after boiling indicates no effect of the heat treatment. The ethylene concentration of the control medium are low as expected.

Additionally, an enzymatic digest with the proteolytic enzyme mix Pronase E was performed. 5 µL of enzyme mix were added to 50 µL of supernatant and incubated at 37 °C over night. The mixture was then tested for ethylene accumulation in *S. pennellii*. The experiment was repeated several times but did not lead to a clear result. There are several possible explanations for this observation: The conditions

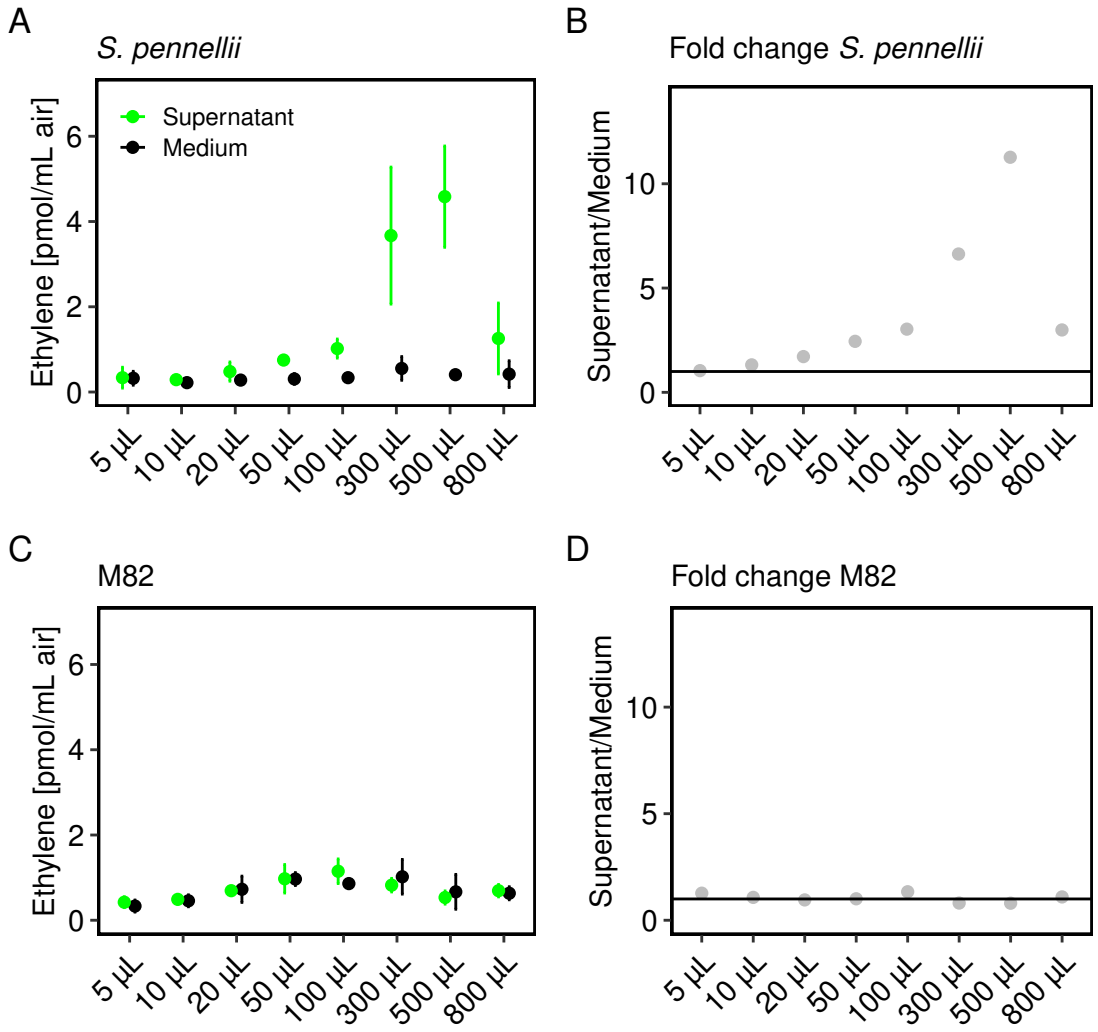

Figure 3.1: Dose dependent production of ethylene caused by the *Rhodanobacter* supernatant (green) compared to the peptone medium (black) as control. Every dot represents the average of 3 replicates +/- S.D.. Grey dots illustrate the calculated fold change (fold change = supernatant/medium). Plant leaf pieces were treated for 4 h. **A**: Ethylene accumulation in *S. pennellii*. **B**: Fold change of the activity in *S. pennellii*. **C**: Ethylene accumulation in M82. **D**: Fold change of the activity in M82. The experiment was repeated three times with similar results.

were not optimal for a digest or the active compound is not of proteinogenic nature. A negative digestion result does not exclude the possibility of a peptide. Cyclisation or the exchange of L- with D- amino acids could also prevent an enzymatic digest.

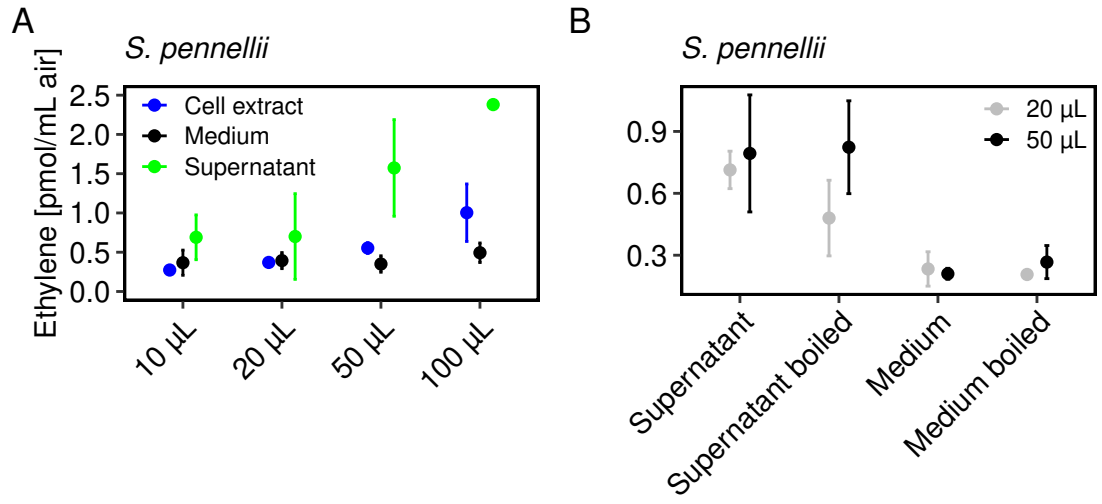

Figure 3.2: Dose dependent ethylene induction of the *Rhodanobacter* cell extract and heat stability of the *Rhodanobacter* supernatant. Every dot represents the average of 3 replicates +/- S.D.. Plant leaf pieces were treated for 4 h. **A**: Ethylene accumulation of the cell extract (blue), supernatant (green), and peptone medium (black) as control. **B**: Heat stability of the *Rhodanobacter* supernatant tested in two volumes 20 µL (grey) and 50 µL (black), compared with peptone medium as control. Both experiment were repeated three times with similar results.

3.2.2 Exclusion of flagellin

As already mentioned before, two different epitopes of flagellin are known to cause PTI in tomato. Preclusion of this ubiquitous bacterial protein, even as contamination, is therefore of major importance. Beside the result of the BLAST data base, a flg22 antagonistic experiment was conducted, Fig. 3.3. Chinchilla et al. [10] described a peptide containing the sequence QRLSTGSRINSAKDD-A-GLQIA, which is capable to block flg22-derived ethylene induction and was provided from Professor Felix. An ethylene assay was performed with the antagonist added 5 min before the supernatant. A concentration of 10 µM antagonist could not block the ethylene induction caused by the *Rhodanobacter* supernatant. This experiment further confirms that the ethylene inducing activity is not based on flg22 perception, excluding also a contamination.

Finally, scanning electron microscopy (SEM) pictures of stained *Rhodanobacter* bacteria were taken, Fig. 3.4. Fimbrial structures were visible, but no flagellae.

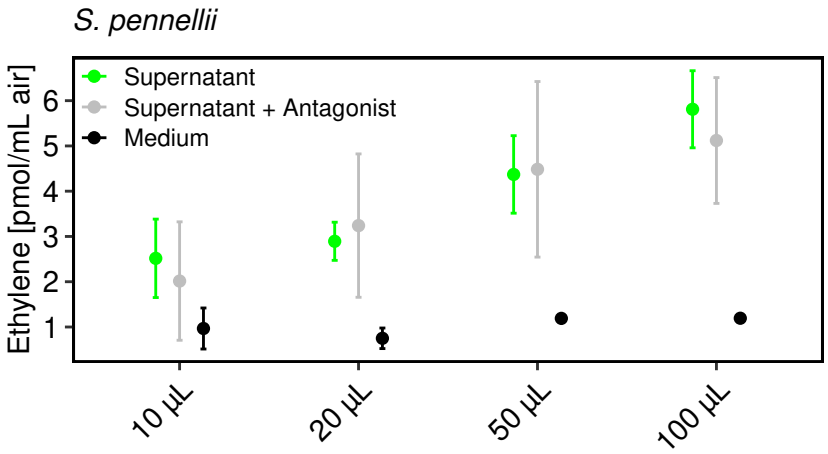

Figure 3.3: Dose dependent ethylene accumulation of untreated *Rhodanobacter* supernatant (green), *Rhodanobacter* supernatant with flg22 antagonist (grey) and peptone medium as control (black). Every dot represents the average of 3 replicates +/- S.D.. Plant leaf pieces were treated for 4 h.

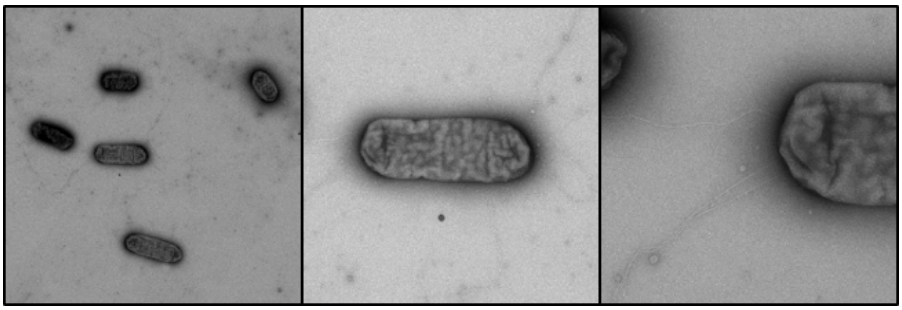

Figure 3.4: Isolated and uranyl acetate stained *Rhodanobacter* bacteria under a scanning electron microscope (SEM) Hitachi S-800. Pictures were taken by Dr. York Stierhof.

Taken together, these results exclude flagellin as elicitor. The comparison with the BLAST data base as well as the SEM pictures consistently show, that the *Rhodanobacter* strain does not possess flagellin. The ethylene assay performed with the flg22 antagonist and the fact that M82 does not react to the *Rhodanobacter* supernatant also exclude flagellin as contamination.

3.2.3 Activity of the *Rhodanobacter* supernatant in *Arabidopsis*

Despite the focus on the tomato system, the *Rhodanobacter* supernatant was also tested in *A. thaliana* ecotype Col-0, hereafter called Col-0. Ethylene biosynthesis was also induced in this model plant, as shown in Fig. 3.5.

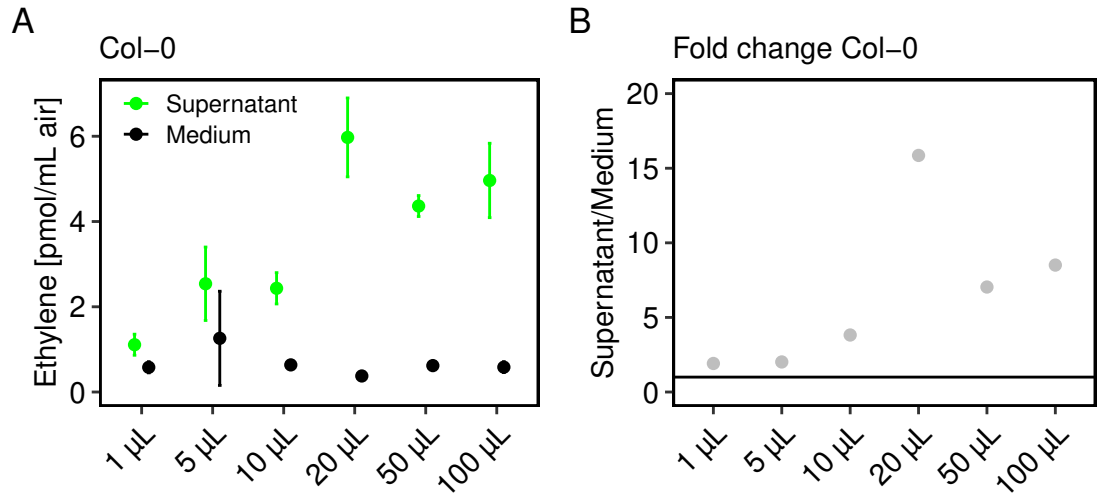

Figure 3.5: Dose dependent ethylene induction of the *Rhodanobacter* supernatant (green) compared to the peptone medium (black) in Col-0. Every dot represents the average of 3 replicates +/- S.D.. Plant leaf pieces were treated for 4 h. **A**: Ethylene accumulation of the *Rhodanobacter* supernatant in Col-0. **B**: Calculated fold change of the activity in Col-0. The experiment was repeated twice with similar results

Although this is an interesting result, it is not comparable to the tomato system. The plants are not related and evolved under different ecological conditions. There might be different sets of receptors. Additionally, the *Rhodanobacter* supernatant did also trigger ethylene accumulation in the *Arabidopsis* mutants sobir1-12 and bak1-5/bkk1. The result is shown in Fig. 3.6. This implies a sobir1 and bak1 independent pathway. A receptor identification could therefore be difficult.

The phenotypic difference between the tomato lines *S. pennellii* and M82 however allows the use of the described mapping population, which facilitates a receptor identification. The purification process was therefore continued in favor of the *S. pennellii*.

3.2.4 Time dependent development of the *Rhodanobacter* derived active substance

To get a high amount of the *Rhodanobacter* derived active substance, a fermentation curve was performed. The strain was cultivated as described in the Method section. Samples were taken in 12 h intervals over a period of five days.

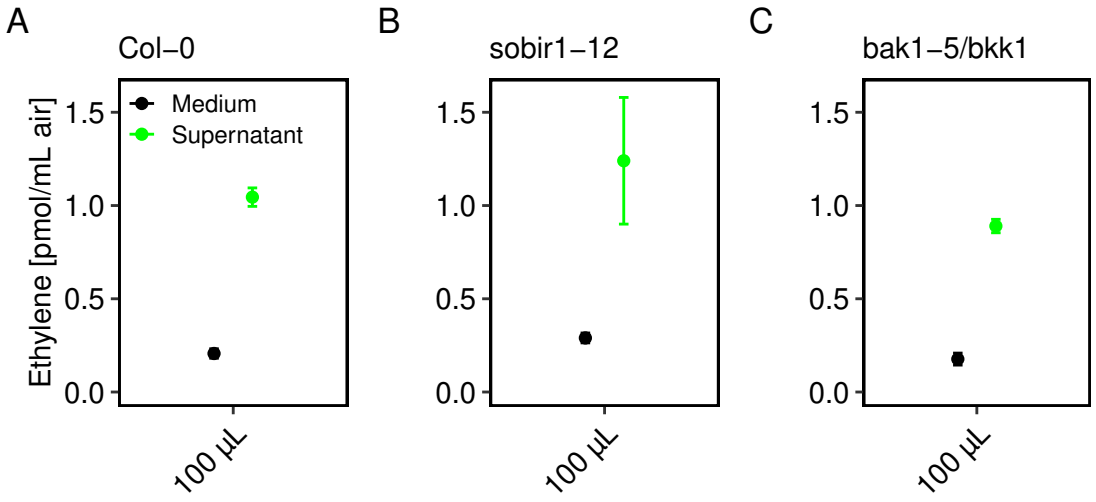

Figure 3.6: Ethylene accumulation of 100 µL *Rhodanobacter* supernatant (green) compared to the peptone medium (black) as control. Every dot represents the average of 3 replicates +/- S.D.. Plant leaf pieces were treated for 4 h. **A**: Col-0. **B**: sobir1-12. **C**: bak1-5/bkk1. The experiment was repeated twice with similar results.

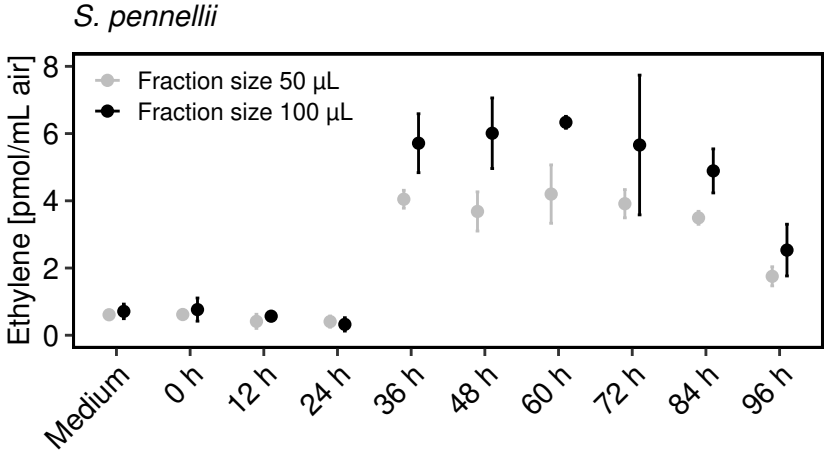

Figure 3.7: Fermentation curve of the *Rhodanobacter* crude supernatant. After inoculation samples were taken in a 12 h interval and tested in two volumes, 50 µL (grey) and 100 µL (black). Peptone medium was used as control. Every dot represents the average of 3 replicates +/- S.D.. Plant leaf pieces were treated for 4 h. The experiment was repeated twice with similar results.

Fig. 3.4 shows the ethylene production of the samples. The activity of the supernatant compared to the medium increased substantially between 24 h and 36 h of cultivation and reached its maximum around 60 h before it starts decreasing. This suggests a constant secretion of activity at the beginning and underlines the activity as bacterial-derived. After around 3 days, when nutrition uptake impedes,

the substance responsible for the activity seems to get digested again. Therefore the supernatant was harvested after 60 h of cultivation.

3.2.5 Separating the activity from the background

Ion exchange chromatography

Ion exchange chromatography (IEC) was performed as described in the Method section. After adjusting the pH to 8.5, the *Rhodanobacer* supernatant with a conductivity of 8 mS/cm was applied on a strong anion exchange column (HiTrap Q Fast Flow, 5 mL). The active compound remained in the flow through. The same was also observed with a strong cation exchange column (HiTrap SP Fast Flow, 5 mL) with pH 5.5. This finding suggested a molecule with a big size/charge ratio. Therefore other purification steps were considered.

Extraction with solvents of different polarity

A solid-liquid extraction experiment was performed with the *Rhodanobacter* supernatant. After lyophilization of the supernatant, 10 g of obtained powder was treated 3 x 30 min with 30 mL of the different solvents: MeOH, EtOH, n-BuOH and CH_2Cl_2. After the extraction process, the solid residues were discarded and the united extracts were dried, resolved in 10 mL water and tested for ethylene accumulation in *S. pennellii*, Fig. 3.8. Untreated supernatant and medium were used as control.
Only the polar solvents MeOH and EtOH were capable to extract the activity. However, compared to the untreated supernatant, the extraction was not very efficient. Additionally, the scale up to bigger extraction amounts caused other issues. Bubble formation due to additionally extracted biotensides made following steps of solvent evaporation challenging.

Protein precipitation

Protein precipitation was performed as next purification step. Ammonium sulfate was added to the supernatant until a concentration of ~4 M. The precipitated protein was separated and resolved in water. The remaining salt was removed

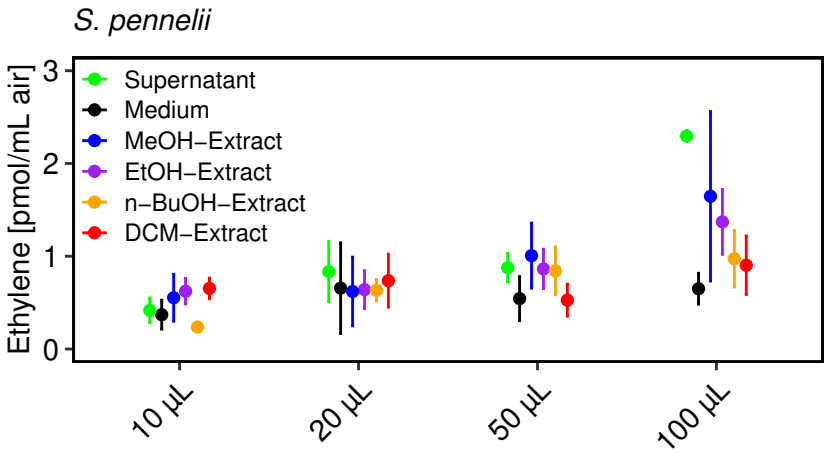

Figure 3.8: Dose dependent ethylene induction of lyophyllized and extracted *Rhodanobacter* supernatant. Extraction was conducted with MeOH (blue), EtOH (purple), n-BuOH (orange) and DCM (red). *Rhodanobacter* supernatant and peptone medium were used as controls. Every dot represents the average of 3 replicates +/- S.D.. Plant leaf pieces were treated for 4 h. The experiment was repeated twice with similar results.

via dialysis (1 kDa cut off). After this process, the sample did not gain ethylene production with this setup Fig. 3.9.

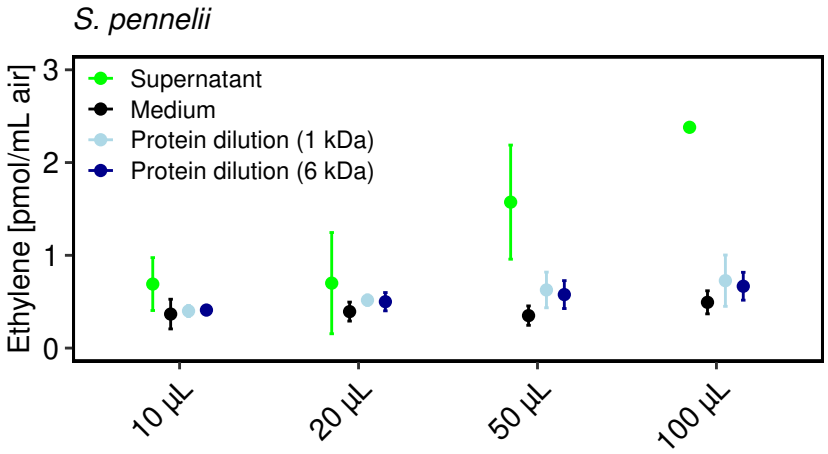

Figure 3.9: Dose dependent ethylene induction of dialysed *Rhodanobacter* protein dilution, after precipitatation from the supernatant. Two membranes with cut off of 1 kDa (grey) and 6 kDa (purple) were used for dialysis. Untreated supernatant (green) and peptone medium (black) were used as controls. Every dot represents the average of 3 replicates +/- S.D.. Plant leaf pieces were treated for 4 h. The experiment was repeated twice with similar results.

This outcome indicates that the activity was either not precipitated or got lost or

inactivated during the process. To examine whether the active substance remained soluble, the remnant solution was also dialysed and tested for ethylene inducing activity, Fig. 3.10.

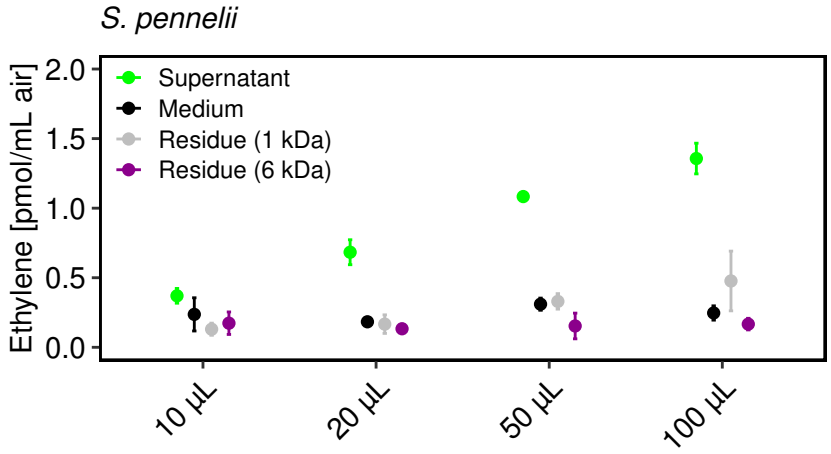

Figure 3.10: Dose dependent ethylene induction of dialysed *Rhodanobacter* residue after protein precipitation. Two membranes with cut off of 1 kDa (grey) and 6 kDa (purple) were used for dialysis. Untreated supernatant (green) and peptone medium (black) were used as controls. Every dot represents the average of 3 replicates +/- S.D.. Plant leaf pieces were treated for 4 h. The experiment was repeated twice with similar results.

As a result, also with higher volumes of sample no activity was detectable. This finding suggests either a small molecule or a protein with a tight folding, capable to pass the dialysis membrane or a inactivation of it. The dialysis approach was therefore dismissed.

Broad spectrum extraction and purification via hydrophobic interaction and size

Another approach to concentrate an activity substance is via hydrophobic interaction. For this, a C18 solid phase extraction column was loaded with *Rhodanobacter* supernatant, washed and eluted with three different mixtures of methanol/water. All fractions were dried and resolved in water and tested with 20 µL and 50 µL for ethylene accumulating activity, Fig. 3.11. Untreated supernatant and medium were used as control.

The ethylene concentration of the supernatant is not very high. A possible explanation for this finding could be the natural variation of the plant state.

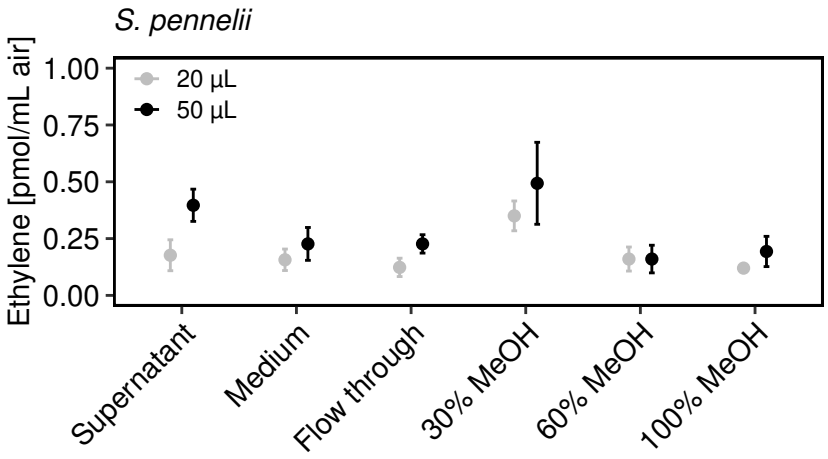

Figure 3.11: Ethylene induction of C18 SPE fractions tested with 20 µL (grey) and 50 µL (black). Elution was done with 30 %, 60 % and 100 % MeOH. *Rhodanobacter* supernatant and peptone medium were used as controls. Every dot represents the average of 3 replicates +/- S.D.. Plant leaf pieces were treated for 4 h. The experiment was repeated twice with similar results.

Nevertheless, some activity was eluted within 30 % MeOH which suggests a rather polar compound.

As an alternative way, an extraction experiment was performed with an hydrophobic Amberlite XAD16 resin. 1 L *Rhodanobacter* supernatant was added to a prepared column containing 100 g of activated resin. The salt was removed by washing with 3 L water and the active compound was eluted with MeOH. After evaporation of MeOH, the remaining solid (12.86 g) was resolved in water with a concentration of 20 mg/mL. The extract was tested in a dose dependent ethylene bioassay Fig. 3.12 A. Untreated supernatant and medium were used as control.

A significant increase in ethylene production was monitored, which suggested the XAD16 resin as favorable method. Fig. 3.12 B shows an enzymatic digest, performed with the Amberlite XAD16 extract and Pronase E enzyme mix. 5 µL of enzyme mix were added to 50 µL of sample and incubated at 37 °C over night. Flg22 incubated with the enzyme mix served as control for a proper activity. To explore whether the enzyme mix can function within the XAD16 extract, an additional flg22 spiking was carried out. As result, Pronase E did successfully degrade the flg22 activity. It did not significantly reduce the ethylene accumulation of the XAD16 extract

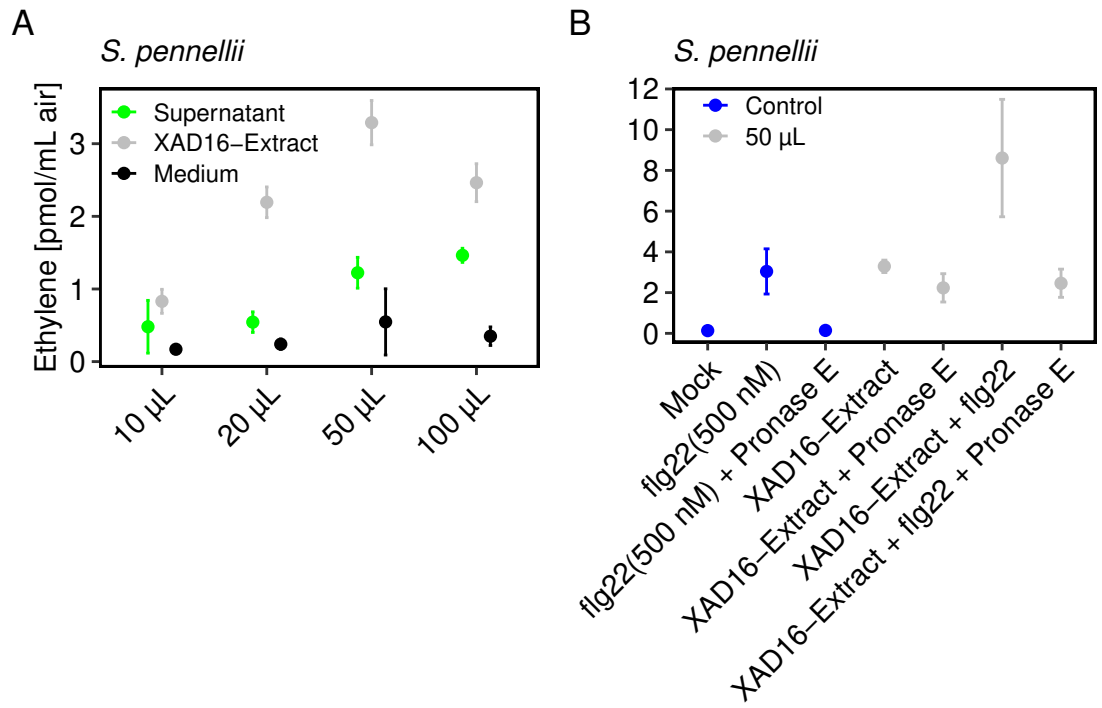

Figure 3.12: Ethylene induction of the Amberlite XAD16 extract. Every dot represents the average of 3 replicates +/- S.D.. Plant leaf pieces were treated for 4 h. **A**: Dose dependend ethylene inducing activity of the extract (grey) compared to *Rhodanobacter* supernatant (green) and the peptone medium (black) as controls. **B**: Enzymatic digest of the XAD16 extract performed with the enzyme mix Pronase E. The experiment was repeated twice with similar results.

(ethylene concentration remained over 2 pmol/mL air), although it degraded the flg22 activity within the XAD16 extract. This result indicates, that the active compound is not sensitive to proteolytic enzymes. The purification step was verified with a silver stained SDS 15 % polyacryl amide gel illustrated in Fig. 3.13. While the *Rhodanobacer* supernatant still contained protein, the Amberlite XAD16 extract did not or only below 10 kDa. This experiment proved the purification protocol as successful process to concentrate and purify the bacterial activity.

3.2.6 Activity purification with size exclusion chromatography

The pre-purified extract was used for a size exlusion chromatographical purification. A glass column was packed with Sephadex LH20 material. 3 mL concentrated XAD16 extract (450 mg/mL) were added to the column. Elution occurred with

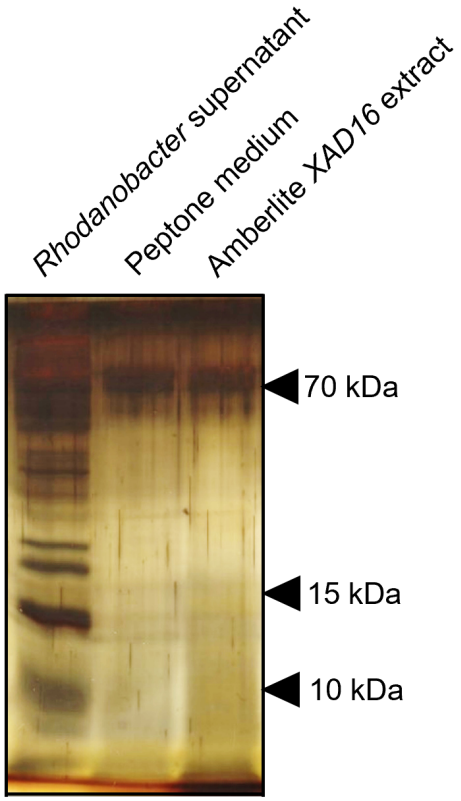

Figure 3.13: Silver stained 15 % SDS polyacryl amide gel. Displayed samples from left to right: crude *Rhodanobacter* supernatant, peptone medium as control and Amberlite XAD16 extract. Protein size was estimated with a prestained protein ladder.

MeOH over night via gravitation. 72 fractions were collected in 15 min intervalls over a period of 18 h. 5 fractions respectively were pooled, dried and resolved in water. A concentration of 1 mg/mL was set and the samples were tested in an ethylene inducing bioassay Fig. 3.14.

The active compound was eluted in fraction 11, after around 14 h, as shown in the graph. Additionally, thin layer chromatography (TLC) was performed to monitor every fraction. Fig. 3.15. displays a selection of active and inactive fractions. The amino acid tryptophan was used as control. It is similar in size and polarity compared to the active compound.

Both molecules could be separated by TLC (C18 RP silica gel 60, F254) with MeOH/H_2O 7:3. While tryptophane has an R_f value of 7,5, a R_f value of 6,9 was determined for the active compound. The isolated active fraction was used

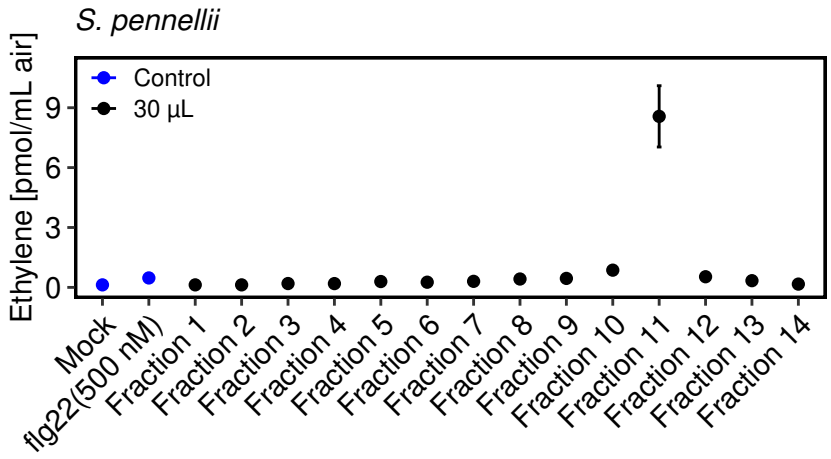

Figure 3.14: Ethylene inducing activity of pooled fractions collected during (Sephadex LH20) size exclusion purification. Every dot represents the average of 3 replicates +/- S.D.. Plant leaf pieces were treated for 4 h. The experiment was performed twice with similar results.

for further purification.

3.2.7 Purification of the activity via semi preparative HPLC

Further purification was performed via High Performance Liquid Chromatography (HPLC) (Thermo Scientific, Ultimate 3000). According to prior information obtained through TLC, a moderate polarity of the active compound could be estimated. This information correlates with the finding of the SPE experiment, which was initially performed Fig. 3.11. The necessary MeOH/H_2O ratio for the elution of the active compound was below 30 % of MeOH, which also indicated a high polarity. A semi preparative C18 column was used for further purification (gradient of 5- 30 % MeOH in 30 min). The absorption was measured with a diode array detector (DAD). Fig. 3.16 shows the absorption spectrum of 210 nm, since the active compound does not show a strong absorption with 280 nm (Fig. 3.18 B) compared to tryptophane.

The HPLC run was repeated eight times to get enough substance (mg) for further experiments. Each run was performed with 1 mL of 1 mg/mL starting material. The respective fractions were pooled and tested for ethylene inducing activity, which is illustrated in Fig. 3.17.

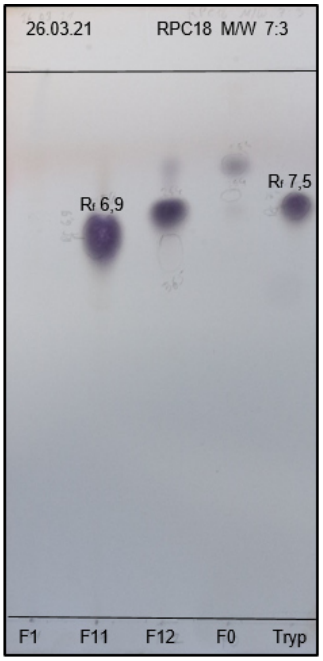

Figure 3.15: Thin layer chromatography of the size exclusion fractions (Sephadex LH20). Tryptophane was used as control. The experiment was performed with a C18 reverse phase silica gel 60, F254 plate (Merck). A mixture of 7:3, methanol/water was used as running solvent. The plate was sprayed with anis aldehyde reagent and developed for 5 min.

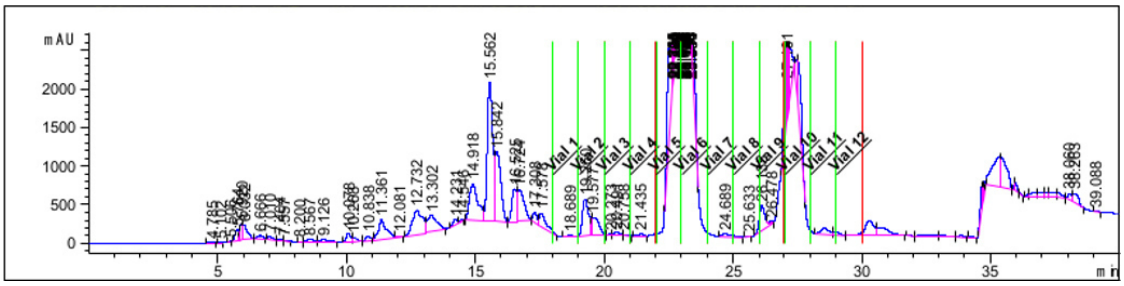

Figure 3.16: Base peak chromatogram of the semi preparative HPLC (C18 column) run. Used gradient: 5-30 % MeOH in 30 min. The absorption was measured with a diode array detector and is displayed at 210 nm. The collected fractions are marked with lines and vial numbers. The vial numbers correspond with the isolated fraction numbers.

The average activity with t_r = 26- 28 min corresponded to vial 9 and 10. The total yield of those two fractions after eight runs was 1 mg. Since the activity correlates to only one peak within the HPLC spectrum, the substance was pure enough for analytical experiments, such as mass spectrometry (MS) for mass determination and nuclear magnetic resonance spectroscopy (NMR) for structural information.

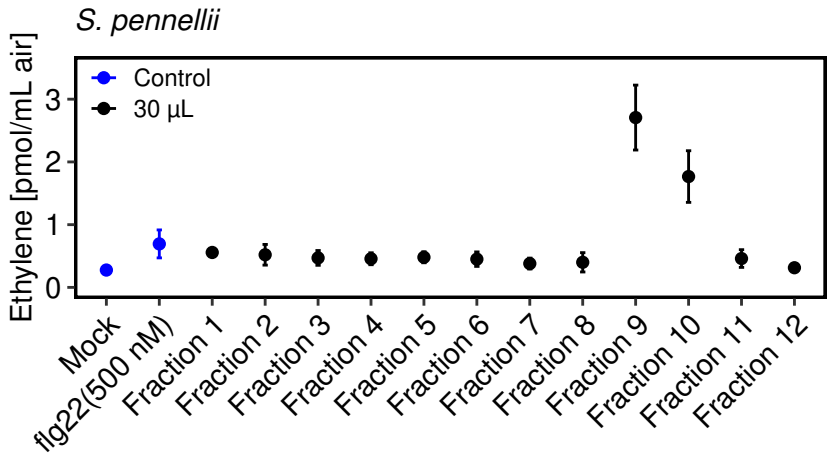

Figure 3.17: Ethylene inducing activity of 30 µL of the collected semi preaparative HPLC fractions. Every dot represents the average of 3 replicates +/- S.D.. Plant leaf pieces were treated for 4 h. The experiment was performed twice with similar results.

3.2.8 Identification of the active compound maculosin

High resolution LC-MS chromatography was used to determine the mass of the substance (gradient 0- 100 % MeOH, 20 min). The elution of the active compound occurred after ~4 min.

With the putative mass of 261,1237 m/z (positive mode), a calculation for the corresponding formula was conducted. The calculation revealed the formula: $C_{14}H_{16}N_2O_3$. Comparison of this formula with the PubChem data base suggested maculosin as compound. The data base further provides structural information about this molecule. The remaining substance was therefore used for a ^{13}C NMR experiment. The obtained NMR spectrum could be directly compared to the literature. Fig. 3.19 shows the shifts of the ^{13}C NMR experiment and the corresponding carbon atoms in maculosin.

All signals were referenced to ^{13}C MeOH. All ^{13}C NMR signals were compared with the ^{13}C NMR signals of maculosin described in the literature [80]. The comparison revealed that maculosin is in fact the molecule of interest. The structure is pictured in Fig. 3.19, (1). Maculosin is a cyclic dipeptide, consisting of L-tyrosine and L-proline. The condensated amino acids form a diketopiperazine structure with a phenol moiety. Compared to tryptophane the π-system of maculosin is smaller,

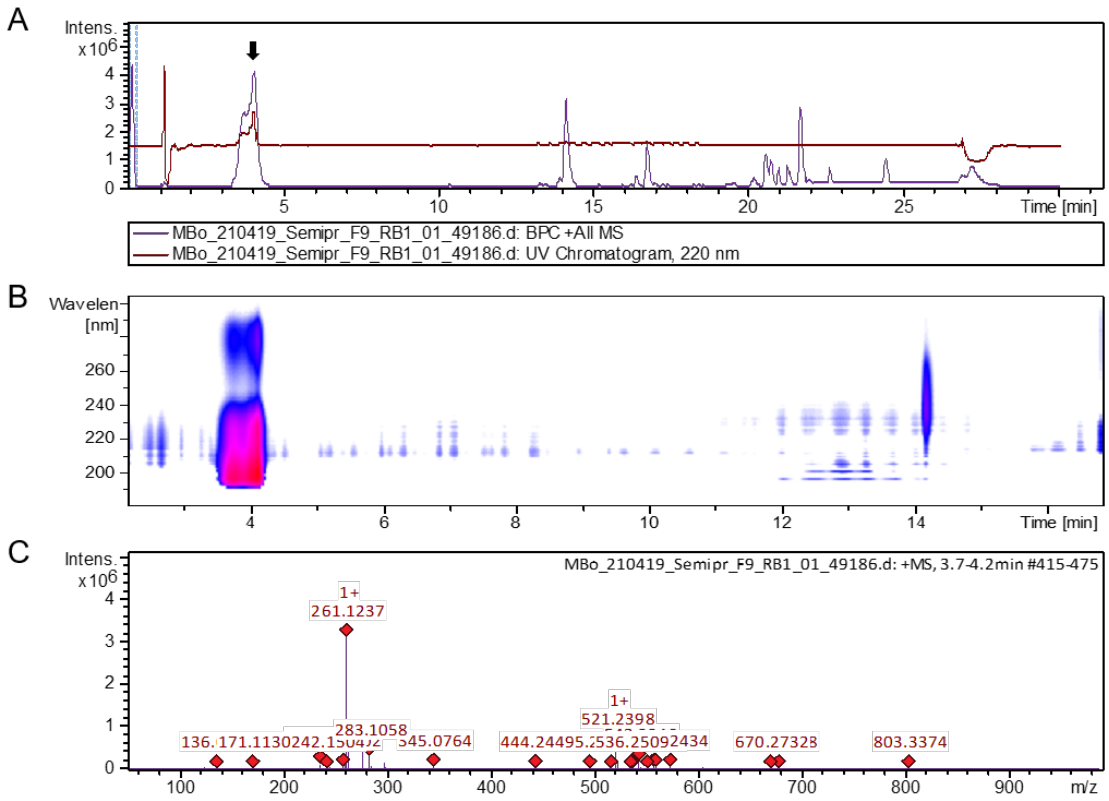

Figure 3.18: (+)MS-Base peak chromatogram and corresponding UV trace of the performed HR LC-MS experiment with fraction 9- 10. **A**: Base peak chromatogram of the analytical C18 HPLC column. The peak of interest is marked with an black arrow. **B**: Absorption spectrum of the eluted compounds. The red color reveals a strong absorption (210 nm), the blue color only weak (280 nm). **C**: Determined mass of the marked peak: 261,1237 m/z (pos. mode).

which explains a weaker absorption at 280 nm. Synthetic maculosin was purchased (Bachem AG, Switzerland) for further experiments. A ^{1}H NMR experiment was performed, to compare the isolated with the purchased maculosin Fig. 3.20. Although the isolated maculosin (blue) is not absolute, all shifts and coupling constants compared to the synthetic maculosin were confirmed.

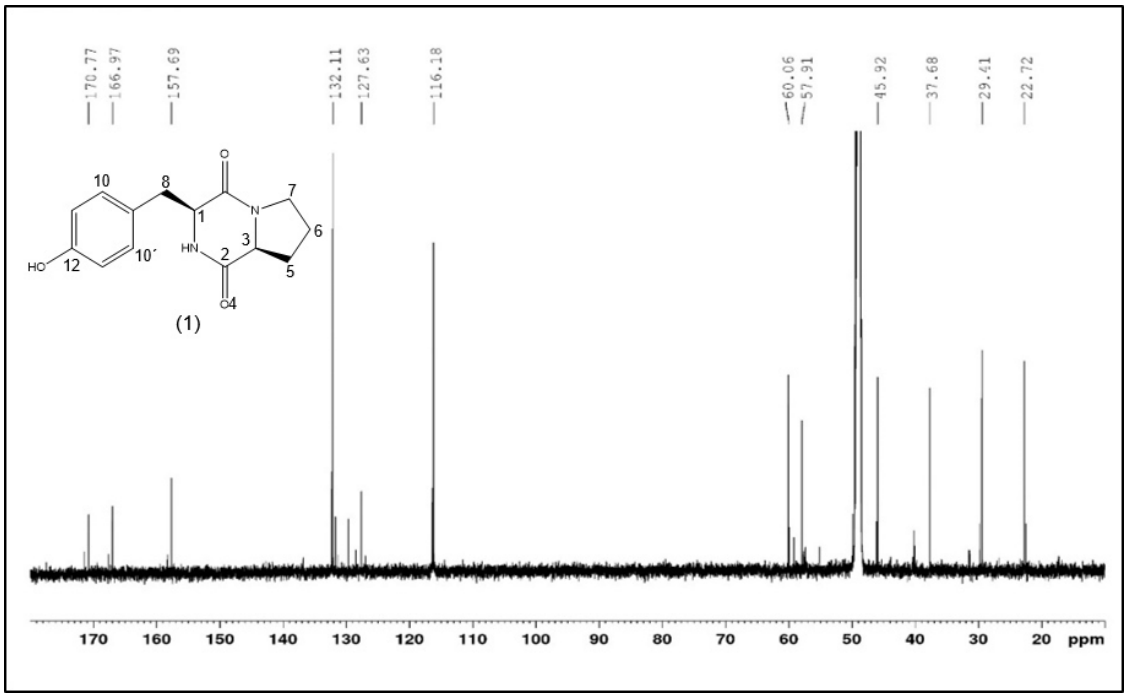

Figure 3.19: 13C NMR (125 MHz, methanol-d4) spectrum of the isolated substance. δC: 170.77 (C-4), 166.97 (C-2), 157.69 (C-12), 132.11 (C-10, C-10'), 127.63 (C-9), 116.18 (C-11, C-11'), 60.06 (C-3), 57.91 (C-1), 45.92 (C-7), 37.68 (C-8), 29.41 (C-5), 22.72 (C-6). Maculosin (1) shows the numbered C-atoms of the corresponding 13C spectrum.

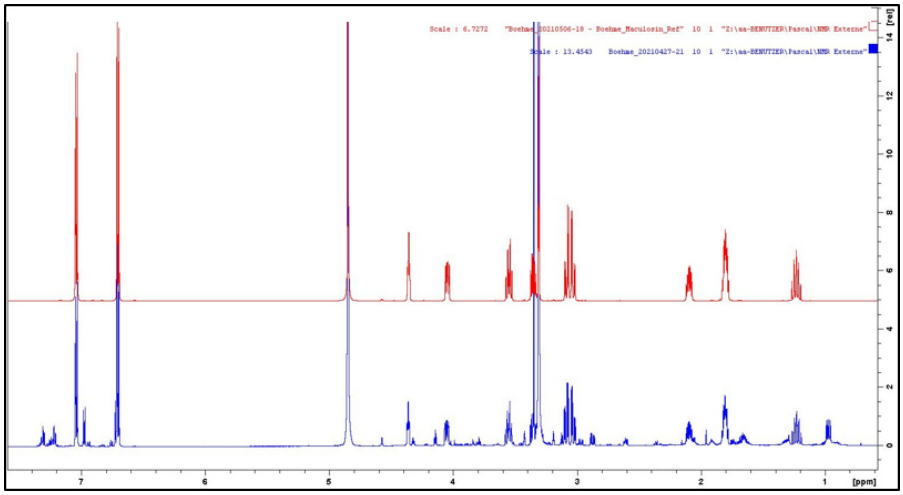

Figure 3.20: Comparison of isolated (blue) with synthesized maculosin (red) via 1H-NMR spectroscopy (Bruker Avance III HDX 600).

3.3 Characterization of synthetic maculosin

Maculosin is described as a host-specific plant toxin, selective against spotted knapweed and produced by the fungus *Alternaria alternata*. The toxin seems to be active only on damaged plant tissue in a concentration range of 10 µM to 1 mM [66]. Immune reactions from other plants are so far unknown. Although there were suggested targets of maculosin (1) [81], the exact molecular mechanism underlying the intoxication remains unclear. In this work, a dose dependent ethylene induction assay as well as a reactive oxygen species (ROS) burst assay were conducted with commercially available maculosin (Bachem Holding AG, Bubendorf) in *S. pennellii*, Fig. 3.21.

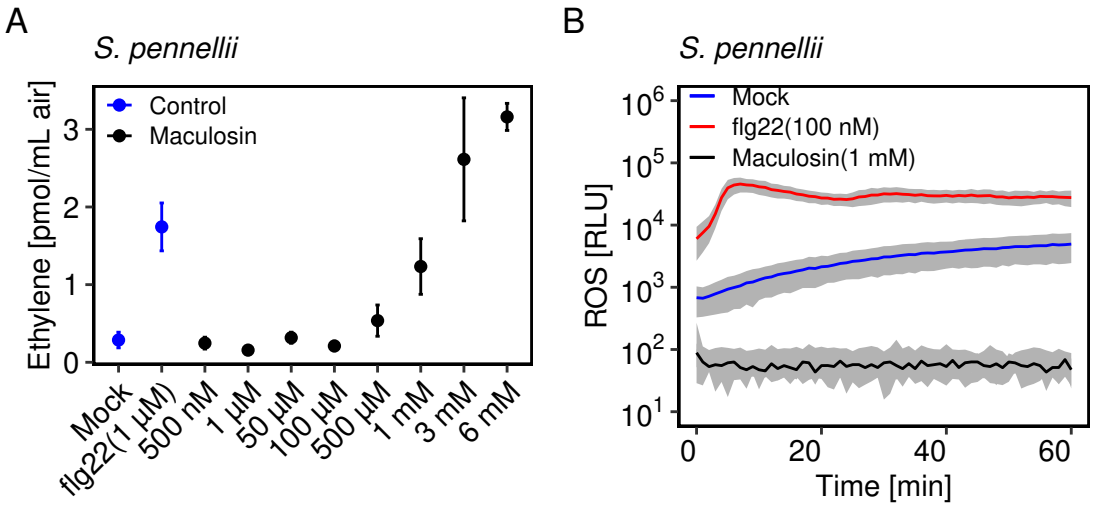

Figure 3.21: Immunostimulant activity of maculosin (1) in *S. pennellii*. **A**: Concentration dependent ethylene accumulation. Every dot represents the average of 3 replicates +/- S.D.. Plant leaf pieces were treated for 4 h. **B**: ROS burst assay with different concentrations of maculosin. The lines represent the avarage of 8 replicates +/- S.D.. Leaf pieces were directly measured after treatment. Both experiments were repeated twice with similar results.

A concentration dependent ethylene production was induced in *S. pennellii*. The required concentration for a significant response hits 1 mM. This is 2000 times higher than for known elicitors, e.g. the active epitope flg22 acts in a nM range [82]. This indicates a mode of action different from that of classical elicitors. Moreover, no ROS burst was elicited. ROS production caused by maculosin is lower than

the water control (mock). A possible explanation is that maculosin (1) acts as scavenger and suppress ROS production [83].

In addition to ethylene and ROS production, a callose deposition assay was performed with maculosin. Leaves of *S. pennellii* were infiltrated with three different concentrations of maculosin (1) (1 mM, 3 mM and 6 mM). The concentrations were chosen because of their significant ethylene induction property. After 72 h, the leaves were harvested and the callose deposition was evaluated, Fig. 3.22 and 3.23.

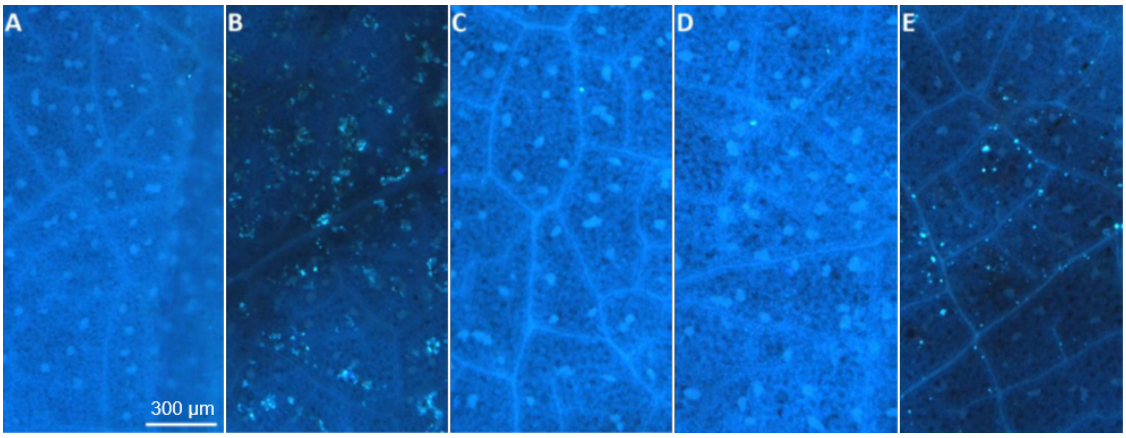

Figure 3.22: Fluorescence pictures of deposed callose. Plant leafs of *S. pennellii* were infiltrated with different concentrations of maculosin, stained with aniline blue and scanned under the microscope. White dots mark the deposed callose. **A**: Infiltrated water (mock). **B**: PEN (5 mg/mL) as positive control. **C**: 1 mM maculosin. **D**: 3 mM maculosin. **E**: 6 mM maculosin. The experiment was repeated three times with similar results.

For quantification, the amount of pixels were counted. A concentration dependent deposition of callose could be observed.

This experiment together with the evaluation was done by Lambrianna Logarnudi under my supervision [84].

Stierle et al. [66] described the formation of necrotic tissue in spotted knapweed after treatment with maculosin in a nicked-leaf bioassay. Due to the unavoidable leaf damage from the infiltration process in the conducted callose deposition assay, one could expect also necrotic tissue formation similar to this described for spotted knapweed. However, no necrosis was detectable in *S. pennellii*, 72 h after inoculation.

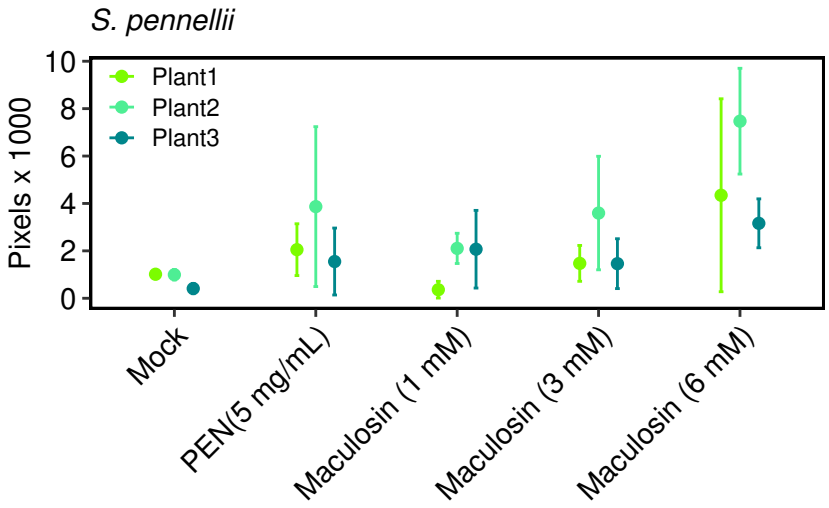

Figure 3.23: Quantitative evaluation of callose deposition in *S. pennellii* after infiltration with maculosin. Results of three infiltrated plants are shown in comparison. Water and PEN(5 mg/mL) were used as controls. Every dot represents the average of 3 replicates +/- S.D..

3.4 Activity of maculosin and some derivates in a variety of different plants

Previous researches, regarding the effect of maculosin in plants, focused on induced necrosis. We have detected ethylene production in the tomato line *S. pennellii*, but no necrosis. Several different plant species were treated with maculosin and the ethylene accumulation was monitored. Fig. 3.24 shows the ethylene induction in 4 different model plants, including other plants of the *Solanaceae* family.

Interestingly, maculosin (1) did not trigger basal immunity in *S. lycopersicum* M82, nor did it in *Arabidopsis* (Col-0) or tobacco. The activity seems thus to be specific to tomato *S. pennellii* as can be detected from the limited number of plant species tested. Even other plants of the same family as *S. pennellii* did not react to the treatment (table 3.2). This finding may have been caused by the adaption in different ecosystems. *S. pennellii* originates in the mountains of south America and has to deal with other environmental conditions compared to the M82 tomato, which was adapted as crop in Europe.

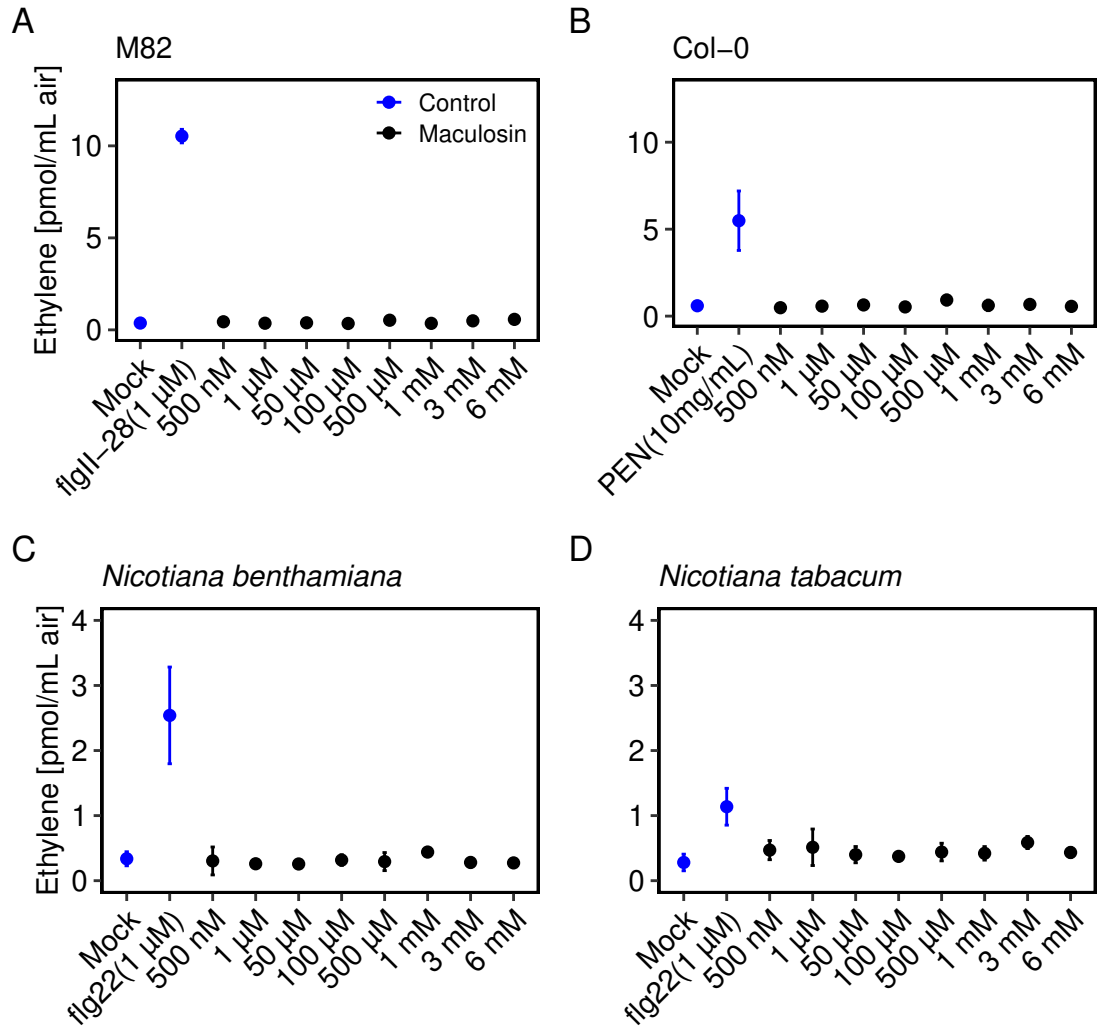

Figure 3.24: Ethylene inducing activity of synthesized maculosin in 4 different model plants. Every dot represents the average of 3 replicates +/- S.D.. Plant leaf pieces were treated for 4 h. The experiments were repeated three times with similar results.

3.4.1 Active moiety of maculosin

Some structural derivates of maculosin were already tested for necrosis formating activity, following the aim to reveal the essential active residue of maculosin [68]. However, other widespread 2,5-diketopiperazines were tested in this study, since there are only few data about this substance group inducing basal immunity. For that purpose one of the two amino acids of maculosin was exchanged to get structure-related, yet different 2,5-diketopiperazines. Fig. 3.25 gives an overview about the structure of the purchased derivates. All of them occur in nature, with

a specific biological relevance [85] [86] [87].

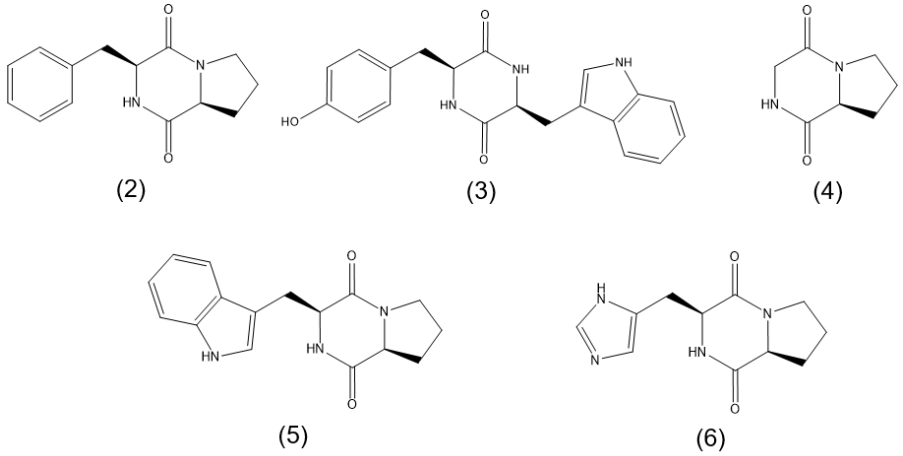

Figure 3.25: Structural formula of the maculosin derivates. **(2)**: Cyclo(L-Phe-L-Pro) (cFP), **(3)**: Cyclo(L-Tyr-L-Trp) (cYW), **(4)**: Cyclo(L-Gly-L-Pro) (cGP), **(5)**: Cyclo(L-Trp-L-Pro) (cWP), **(6)**: Cyclo(L-His-L-Pro) (cHP). All molecules belong to the group of 2,5-diketopiperazines.

Other plants included in this study were chosen following the earlier study of necrosis induction and according to their availability. Table 3.2 contains an overview of the used plant species and the result of the ethylene bioassay. Screening was performed by Lambrianna Logarnudi under my supervision [84].

Table 3.2: Plant species screen with different 2,5-diketopiperazines

Plant species	**cYP**	**cFP**	**cGP**	**cHP**	**cWP**	**cYW**
Solanum pennellii	✓	X	X	X	X	X
Solanum lycopersicum cv. M82	X	X	X	X	X	X
Arabidopsis thaliana Col-0	X	X	X	X	X	X
Lotus japonicus	X	X	X	X	X	X
Brassica napus	X	X	X	X	X	X
Brassica oleracea	X	X	X	X	X	X
Solanum tuberosum (Désiréé)	X	X	X	X	X	X
Centaurea stoebe	X	X	X	X	X	X
Centaurea cyanus	X	X	X	X	X	X
Capsicum annuum	X	X	X	X	X	X
Helianthus annuus	X	X	X	X	X	X
Lactuca	X	X	X	X	X	X
Marian thistle	X	X	X	X	X	X
*Solanum lycopersicum**	X	X	X	X	X	X

*Aunt Ginny´s purple tomato

Maculosin induced basal immunity specifically in *S. pennellii*. No other tested derivate showed activity in the range between 500 nM and 6 mM, including *Centaurea stoebe*, the plant which is known for necrosis formation after maculosin treatment. Considering the occurrence of 2,5-diketopiperazines and their range of known biological effects this is rather surprising. Also cyclo(L-Phe-L-Pro) (2) did not show an induction of ethylene biosynthesis, although the difference from maculosin is only one hydroxy group. This result highlights the specificity of molecular recognition from the plant side. Apparently, a structure backbone is not sufficient to elicit a response, as it is for example for auxin derivates [85]. Already one functional group makes the difference in ethylene production for (1).

3.5 Origin and activity of maculosin in tomato and *Arabidopsis*

Maculosin is a characterized molecule of different origin. Beside fungi like *Alternaria alternata* [66] or *Botryodiploidia theobromae* [88] and bacteria for example *Pseudomonas putida* [89] or *Lysobacter capsici* [67], maculosin is also present in peptone medium [90]. Peptone medium was used in this study as culture broth for the cultivation of the *Rhodanobacter* strain. To clarify whether maculosin is originated from the medium or is bacteria derived, the samples of the *Rhodanobacter* fermentation curve (Fig. 3.7) were investigated for their maculosin content. The fermentation samples of crude *Rhodanobacter* supernatant were therefore analyzed by LC-MS. Fig. 3.26 A displays the base peak chromatogram of F0- F8 with untreated peptone medium as control (red line).

The Mass spec chromatogram does not show absolute concentrations of different substances. However, comparable is the area of peaks with the same r_t. Bigger areas roughly imply higher concentrations. Lines in the front of the graph represent samples in the beginning of the fermentation (F0). Backward lines represent the content of the proceeded fermentation process. No ethylene accumulation was induced in the samples F0- F2, high ethylene accumulation was detected in F3-

F6, Fig. 3.7. Over time, a compound transformation is visible. While the polar substances r_t 1- 6 min did not change much, more hydrophobic substances seem to change in their concentrations. In contrast to signals with r_t 11- 12 min which decreased over time, signals with r_t 21 min increased.

A specific search for maculosin in every sample is possible with the information of mass and r_t. Fig. 3.26 B shows the extracted base peak chromatogram of the samples F0- F7. Peak area and shape of the samples indicate the same quantitative amount of maculosin in every sample (F0- F7). This finding suggests maculosin as medium-derived, since there is no increase of the peak area over time.

The dose dependent induction of ethylene of the *Rhodanobacter* supernatant, which was found in the initially performed screen does not fit to this result. Fig. 3.1 and Fig. 3.7 clearly indicate a bacterial-derived elicitor. However, macuolsin seems to behave similar to this yet unknown elicitor as trigger of ethylene synthesis in *S. pennellii* but not in M82. The concentration of maculosin at the beginning, in the used peptone medium, was to small to have an ethylene inducing effect in *S. pennellii*. During the purification process, the initially found activity must have decreased while the concentration of maculosin increased until a detectable level. Since no second active peak was visible during later stages of purification, it is likely that this change happened while extraction of the crude supernatant within one purification step. This progress remained unrecognized, because it is hardly possible to distinguish two unknown elicitors within one sample with an ethylene assay. Natural variation in the plant state caused differences in the ethylene response and additionally impairs a clear distinction.

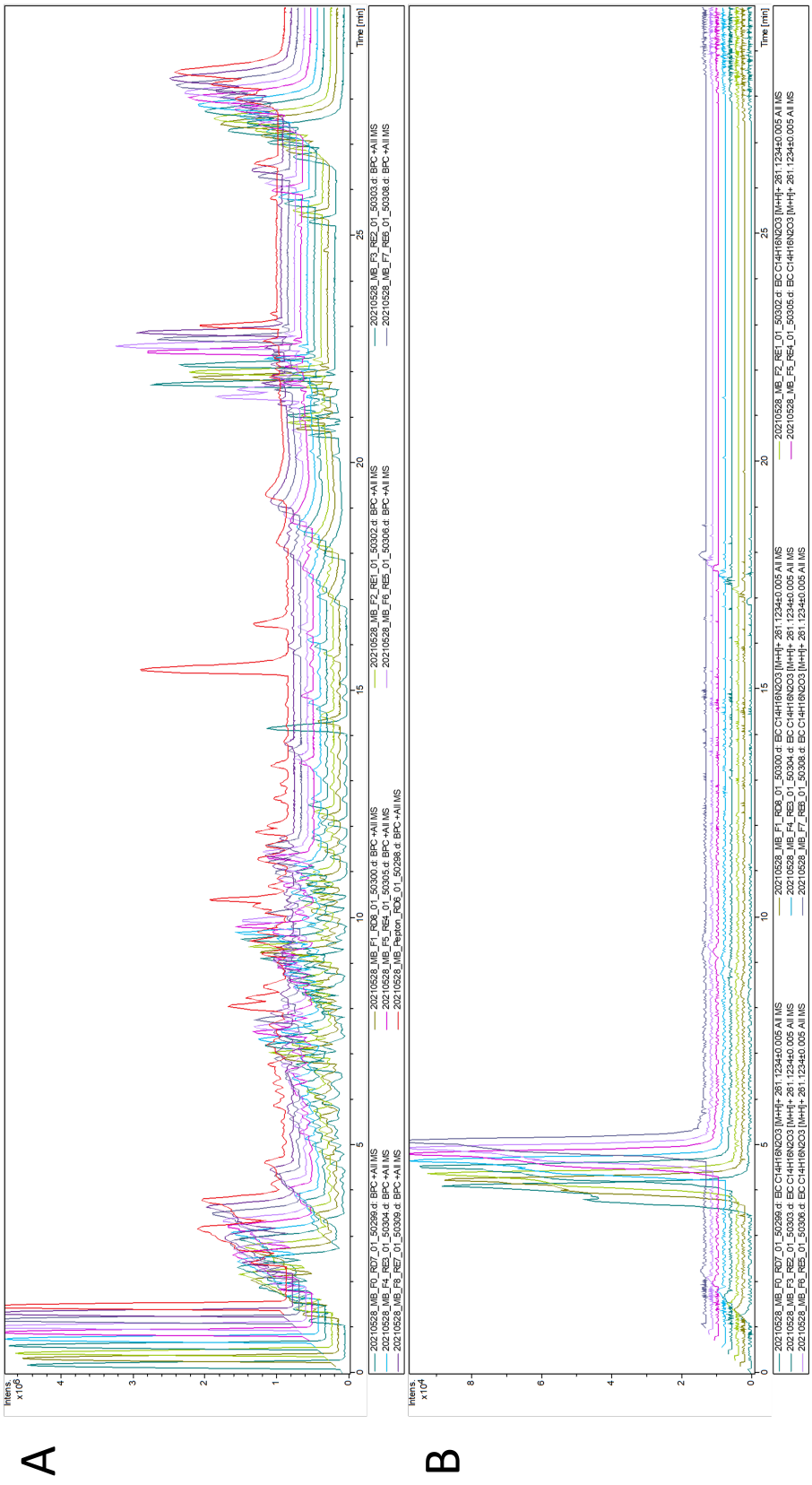

Figure 3.26: **A**: Base peak chromatogram of the fermentation curve samples F0 - F8 with peptone medium as control. Colored lines represent the different samples. **B**: Extracted base peak chromatograms of the samples F0- F7 for relative maculosin evaluation.

3.6 Screen of the introgression line mapping population between *S. pennellii* and M82

As already mentioned above, a target for maculosin (1) is controversial. To narrow down the location of the target, the backcross introgression line mapping population between *S. pennellii* and M82 was screened [75]. The population consisted 45 lines with a M82 backbone and *S. pennellii* insertions. Due to the difference in basal immunity induction, only the introgression line with the insertion including the maculosin target is supposed to react to the treatment. The experiment was performed by Lambrianna Logarnudi under my supervision [84].

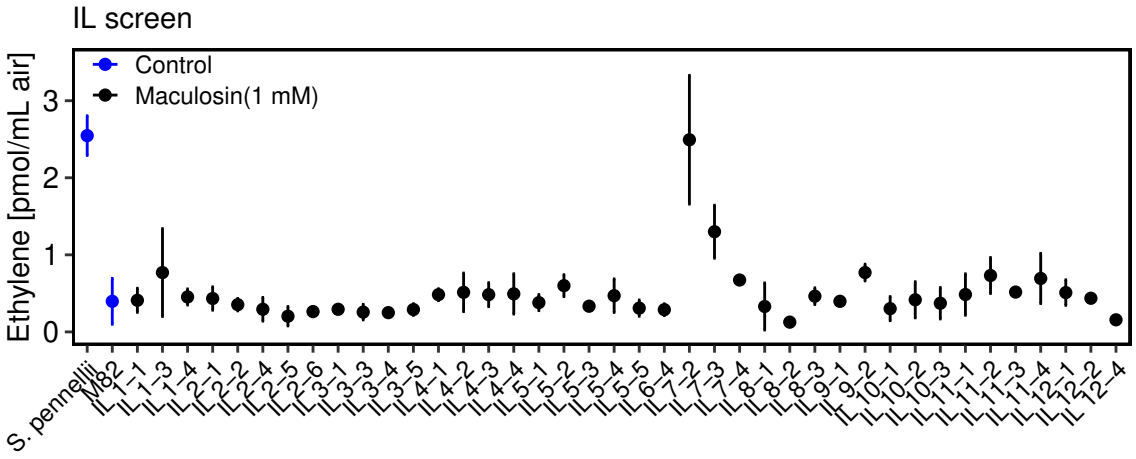

Figure 3.27: Ethylene inducing screen of the mapping population with maculosin. The two tomato lines *S. pennellii* and *S. lycopersicum* M82 were used as control. Every dot represents the average of 3 replicates +/- S.D.. Plant leaf pieces were treated for 4 h. The whole screen was done once. Lines with a ethylene response were repeated two times, with similar results.

As shown in Fig. 3.27 the target is located on chromosome 7 insertion 2 and 3. The related lines show a clear ethylene induction. This observation is reasonable, since those insertions are overlapping, Fig. 3.28. For identification of the maculosin target, further research is necessary. What can be concluded is that maculosin targets not a canonical plasma membrane immune receptor, which would make an identification via mapping population difficult.

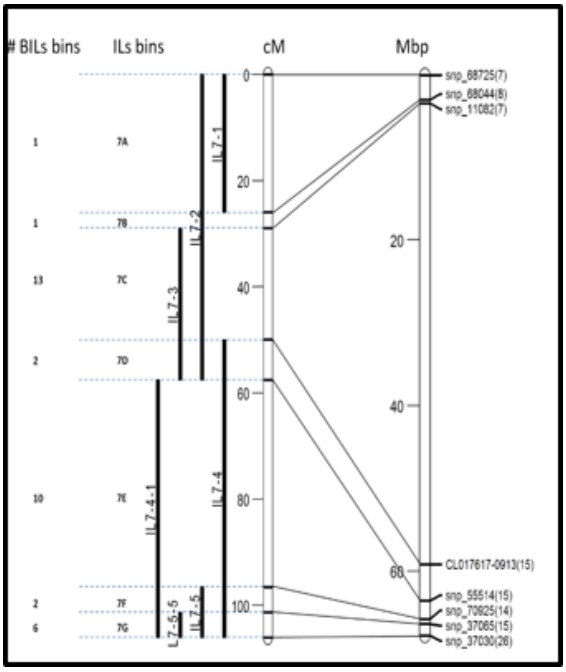

Figure 3.28: Graphical representation of the tomato chromosom 7. Beside physical and a genetical map, the insertions of *S. pennellii* in M82 are shown and marked from IL 7-1 until 7-5-5.

3.7 Activity based purification of an *Ensifer* (2G2) supernatant

The initial performed screen (Chapter 3.1) also revealed significant ethylene inducing activity in the strain *Ensifer* (2G2). The bacteria were grown for three days in peptone medium. Cells were separated and the supernatant was tested in a concentration dependent ethylene bioassay. The peptone medium was used as control. Ethylene production induced by different volumes of supernatant are shown in Fig. 3.29. While a difference between supernatant and medium is visible in *S.pennellii*, no significant difference is shown in M82. The calculated fold change shows the factor of the activity/background ration. Also higher volumes of medium do not elicit significant ethylene production which indicates a bacterial-derived active molecule. This observation together with the assumption that this strain does not develop flagella (according to the BLAST data base) excludes all known bacterial elicitors for tomato including medium-derived maculosin as toxin. Further purification steps were performed using the *Ensifer* supernatant.

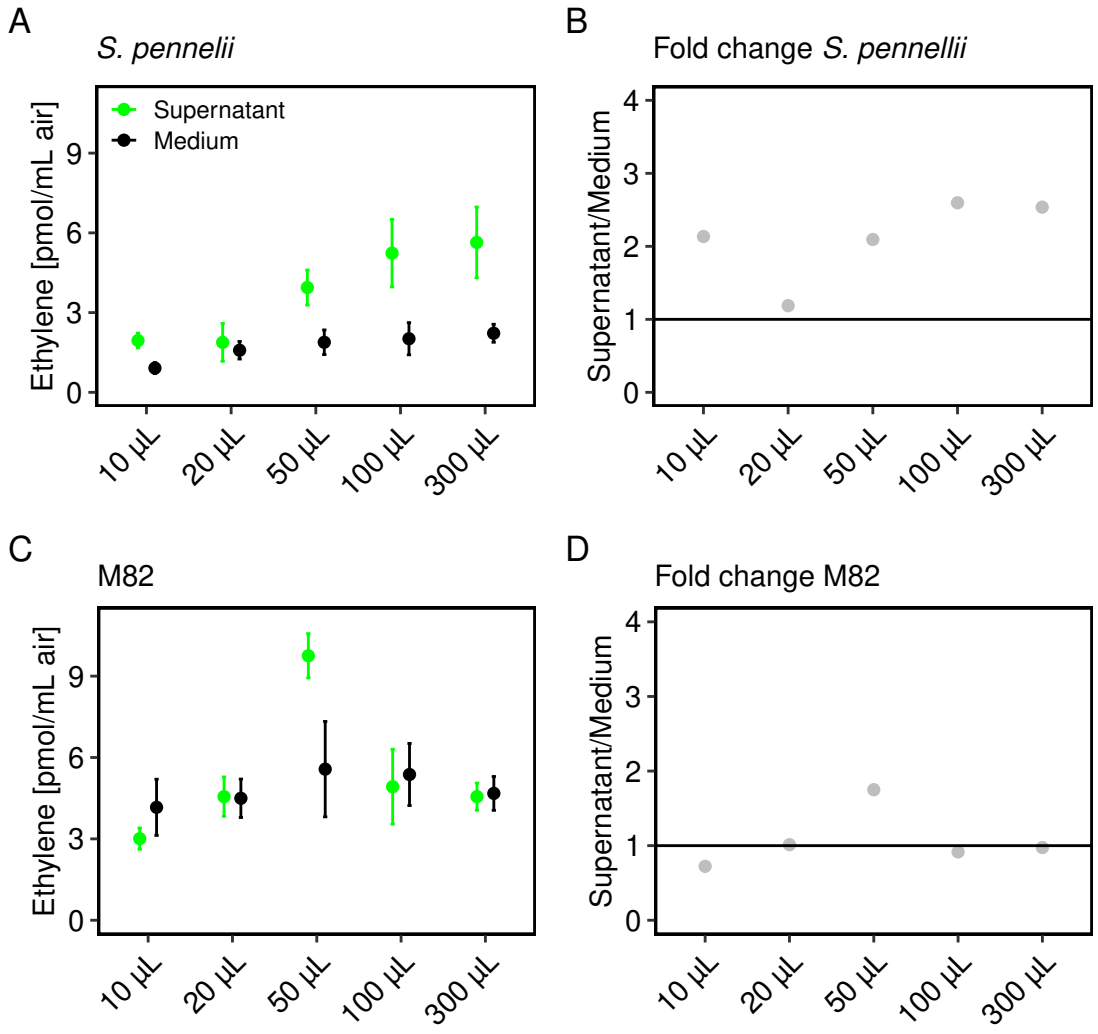

Figure 3.29: Dose dependent production of ethylene caused by the *Ensifer* supernatant (green) compared to the peptone medium (black) as control. Every dot represents the average of 3 replicates +/- S.D.. Grey dots illustrate the calculated fold change (fold change = supernatant/medium). Plant leaf pieces were treated for 4 h. **A**: Ethylene accumulation in *S. pennellii*. **B**: Fold change of the activity in *S. pennellii*. **C**: Ethylene accumulation in M82, **D**: Fold change of the activity in M82. The experiment was repeated three times with similar results.

3.8 Protein precipitation and purification

The whole purification process was performed by Lambrianna Logarnudi under my supervision and can be reviewed in her Bachelor thesis [84]. The following sections only provide a summary of the purification protocol, including some key steps.

A protein precipitation with 2 M ammonium sulfate was performed. The protein

pellet was separated via centrifugation and resolved in water. Desalting was done with a C18 solid phase extraction (SPE, C18, 10 g, Chromabond) column. Elution occurred with 60 % methanol. After evaporation of the solvent, the pellet was resolved in 40 mL water and applied on a strong anion exchange column (HiTrap Q Fast Flow, 5mL). Fig. 3.30 shows the obtained elution profile. A three step gradient was used for a first separation. All fractions contained 25 mL and were tested for ethylene induction. Ethylene triggering activity was found for fraction A1 in both tomatoes *S.pennellii* and M82 and for fraction A2 only in *S. pennellii*. Since a different phenotype between the tomato lines is necessary to use the mapping population, further purification was conducted with A2. The focus on *S. pennellii* additionally excludes the csp as eliciting protein [79].

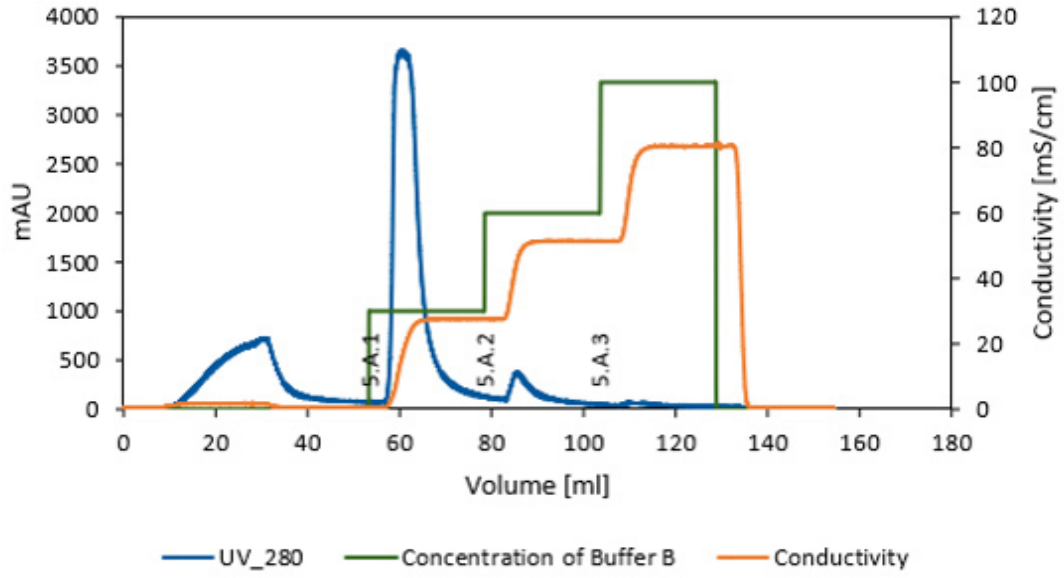

Figure 3.30: Elution profile of the anion exchange chromatographical purification of the *Ensifer*-derived protein. Absorption was measured with 280 nm (blue). Elution was performed with a 3 step gradient (green). Conductivity is displayed in orange.

The whole purification process was monitored with a silver stained 10 % SDS polyacrylamid gel, Fig. 3.31. The anion exchange fractions contain less protein than the crude supernatant. Fraction A1 contains an isolated band around 35 kDa, whereas fraction A2 contains no bigger proteins. However, with a 10 % SDS polyacrylamid gel, no proteins or peptides smaller than 10 kDa can be monitored.

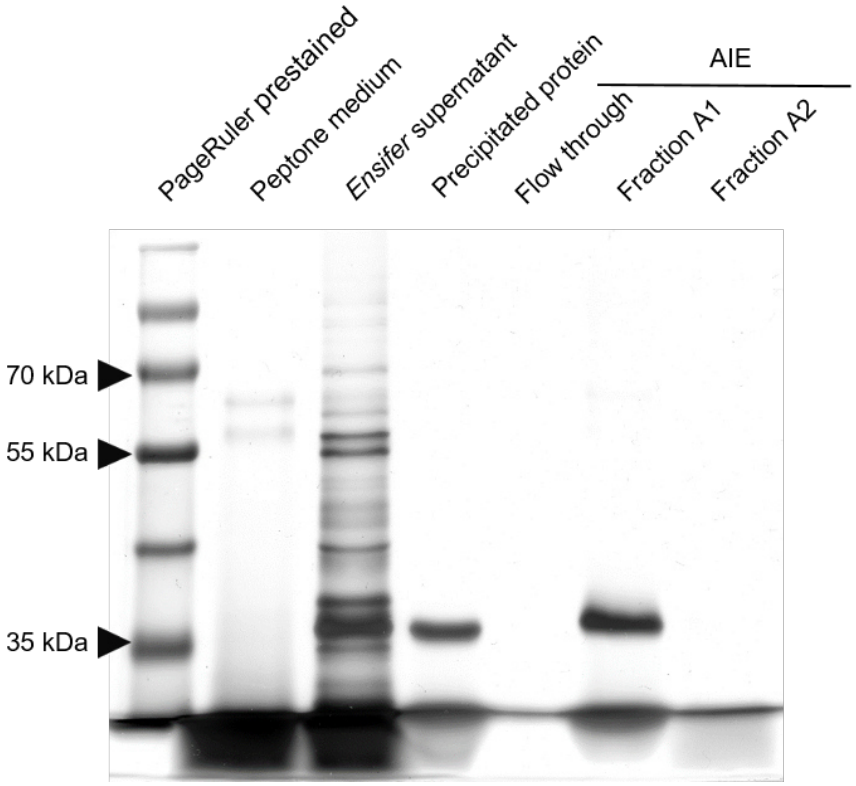

Figure 3.31: Silver stained 10 % SDS polyacrylamid gel with obtained fraction of the anion exchange chromatography, compared to the crude supernatant and peptone medium as control.

Fraction A2 was dialysed against the buffer A for cation exchange chromatography. A membrane with cut off of 1 kDa (Spectra/Por 6, Specturm labs) was used. Fraction A2 was applied to a strong cation exchange column (HiTrap SP Fast Flow, 5 mL). For better separation, a linear gradient was used. Fig. 3.32 shows the obtained elution profile. A low absorption at this length suggests that there are only few peptides with conjugated double bonds, such as aromatic rings.

All obtained fractions were tested for ethylene induction, which occurred in the fractions between 42- 52 % buffer B. Those fractions were pooled. The pooled fractions elicit significant ethylene production, which can be monitored in Fig. 3.33. Additionally, experiments for heat stability and an enzymatic digest were performed.

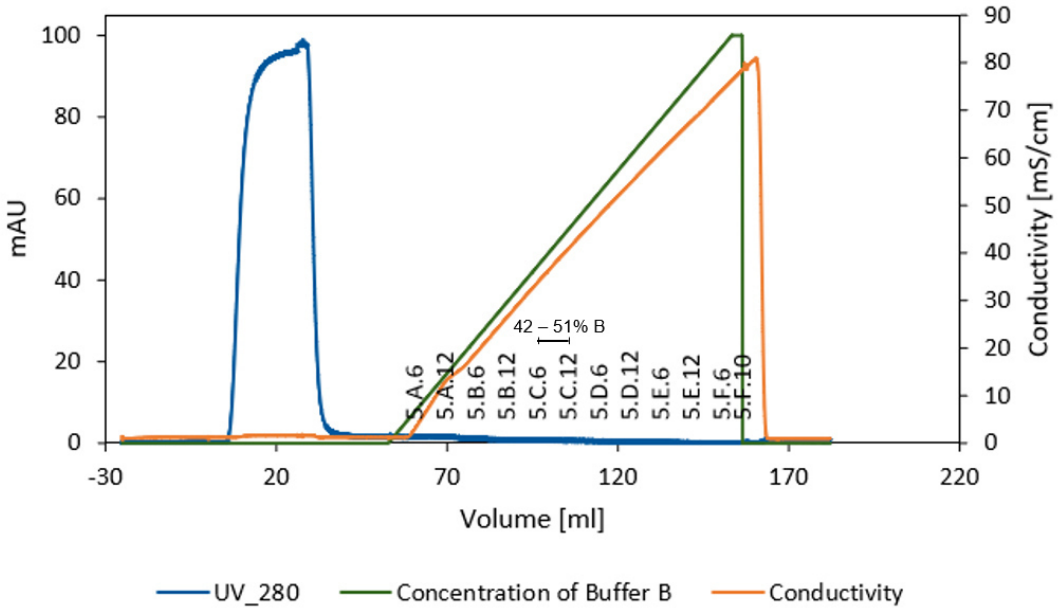

Figure 3.32: Elution profile of the cation exchange chromatographical purification of the *Ensifer*-derived active substance. Elution was performed with a linear gradient (green). Absorption was measured with 280 nm (blue). Conductivity is displayed in orange. The arrow marks ethylene eliciting fractions (42- 52 %).

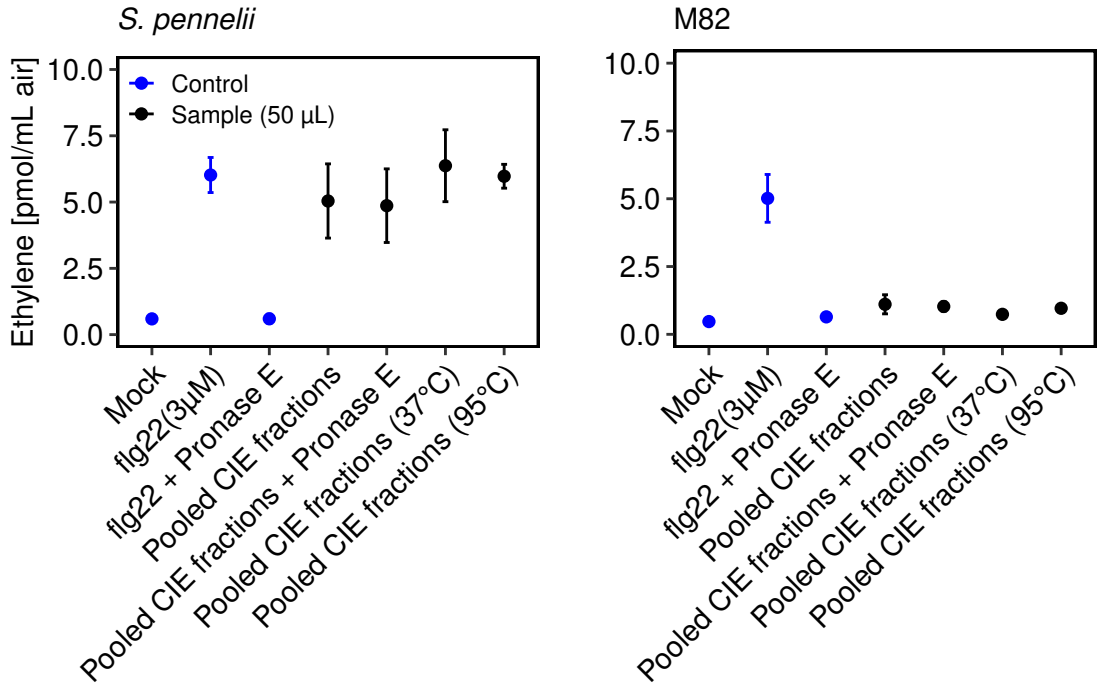

Figure 3.33: Enzymatic digest with the Pronase E enzyme mix and heat treatment of pooled cation exchange fractions. Every dot represents the average of 3 replicates +/- S.D.. Plant leaf pieces were treated for 4 h.

Pronase E treatment did not lead to a decreased activity. Also boiling did not influence the immune response. As mentioned above, many reasons can lead to a negative digestion result. Since, big proteins are more sensible to get degraded under harsh conditions, both findings support the idea of an active molecule smaller than 10 kDa.

Taken together, these findings suggest a small, *Ensifer*-derived molecule, which induces ethylene production in *S. pennellii* but not in M82. Binding neither to a anion- nor to a cation exchange column was possible. However, more effort is needed to identify the active compound.

4 Discussion

Contents

4.1 One molecule, many questions

The final isolated substance was the medium-derived cyclo(L-Tyr-L-Pro), also known as maculosin (1). Maculosin induced ethylene production as well as callose deposition in *S. pennellii*. Although this molecule is already known to be present in peptone medium [90], it is also found as secondary metabolite of various microbes

e.g. bacteria [91] and fungi [66] and could therefore have a deeper, yet unknown function in plant-microbe interaction. We could show, that maculosin acts as activator of basal immunity in *S. pennellii*, and that it is therefore not restricted to spotted knapweed in affecting leaf health. Comparison of maculosin with five derivates revealed insights in the essential active structure. Finally the target location of maculosin could be restricted to chromosome 7 *S. pennellii*. A screen of different plants highlights the specificity of maculosin recognition.

4.1.1 The group of diketopiperazine

Maculosin belongs to the group of cyclo dipeptides (CDPs) or 2,5-diketopiperazines, a large and ubiquitous group found in nature [92]. The simplest form of this group consists of two amino acids. Their cyclic form makes them more stable e.g. against heat and proteolysis. First, CDPs were mainly considered as side products in protein and polypeptide hydrolates or fermentation broths. However, research of the last two decades reveals microbes across different kingdoms are producing this class of substances in general and maculosin in particular, which indicates already a more important biological relevance. Additionally, more and more 2,5-diketopiperazines were found to exhibit diverse biological and pharmacological characteristics [93] [94]. It is also well-established that CDPs can affect plants in various ways. E.g., Cyclo(L-Gly-L-Pro) which was used in this study, is already described to cause extracellular alkalization and ROS production in a tobacco cell suspension [86]. Cyclo(L-Pro-L-Pro) is known to induce systemic resistance in *N. benthamiana* [86]. Other studies show CDPs like cyclo(L-Pro-L-Val), cyclo(L-Pro-L-Phe) and cyclo(L-Pro-L-Tyr) as important signal molecules in bacteria-plant communication and root development [87] [85].

4.1.2 Occurence and properties of maculosin

The occurrence in multiple organisms and inconsistent effects on plants makes the biological relevance of maculosin controversial. While Stierle et al. [66] described it as host specific phytotoxin, which induces necrotic lesions in *Centaurea maculosa*

(renamed to *Centaurea stoebe*), Ortiz-Castro et al. [85] highlighted the plant growth promoting effect of maculosin. Beside that, it is also considered as quorum sensing signal molecule, influencing the plant-microbe interaction by altering the bacterial swarming behavior [95].

Plant growth promotion

Indeed, plant growth-promoting bacteria like for example *Bacillus subtilis* [91], *Lysobacter capsici* AAZ78 [67] and *Pseudomonas putida* WCS358 [96] are known to produce maculosin. Taking the plant pathogens into account, which were found to produce maculosin: *Alternaria alternata* [66], *Leptographium qinlingensis* [97] and *Fusarium nivale* [67], an intended plant growth-promoting effect seems rather questionable. Additionally, also marine organisms were found to produce maculosin [98] [99]. In those cases, maculosin seems to have other biological functions. Another explanation for the root growth promoting effect of maculosin is the auxin recognition system itself. Over 200 substances are known as activators of this auxin receptor transport inhibitor response1 (TIR1). They only have a planar aromatic ring structure and a carboxyl group containing side chain as shared backbone. A single atom attached to the ring can dictate the activity. [85] [100]. Therefore, the weak auxin effect perhaps occurs as side effect.

Phytotoxic activity

Phytotoxins can be classified as pathotoxins or vivotoxins [101]. While pathotoxins are necessary for the virulence and act in very low concentrations, vivotoxins are causing symptoms, but are not required for the virulence [102]. Maculosin causes necrotic lesions in spotted knapweed [66] as well as ethylene production and callose deposition in *S. pennellii*, but in summary, it does not kill the plant [68]. Therefore it could be assigned as vivotoxin. Vivotoxins are in general nonselective [101]. Regarding the toxicity, this is not the case for maculosin, with only two known susceptible plants: *C. stoebe* and *S. pennellii*. A toxic effect could also be determined by the situation. E.g. siderophores are produced by plant growth-promoting

rhizobacteria (PGPR) to complex environmental iron and therefore impede the growth of pathogens [103]. However, siderophores can also act as virulence factors, when secreted by a plant invading fungi [58]. Beside that, siderophores can also induce plant systemic resistance. Applied on plant roots, pseudobactin induces ISR in *Arabidopsis*. [104]. Maculosin could act similar, depending on the application.

Quorum sensing signaling

Bacterial pathogens and symbionts rely on QS signaling to colonize their hosts. QS molecules are autoinducers which regulate the population-dependent gene expression in bacteria. The most common QS class of substances in Gram-negative bacteria are N-acyl homoserine lactones (AHLs). The accumulation of AHLs in nanomolar to micromolar concentrations elicits many functional responses from the plant side [105]. The induced responses are further dependent on structure, concentration and time of exposure, suggesting putative AHL receptors in plants [106].

Some CDPs including maculosin, seem to have similar physicochemical properties, especially to short chain AHLs. They are found to interfere with the AHL-mediated swarming modality, although they act in millimolar concentrations [95]. It is therefore possible that plants react to higher concentrations of maculosin or other CDPs similar as to AHL signal molecules.

Beside AHLs, other QS molecules are described as elicitors. The bacterial fatty acid *cis*-11-methyl-2-dodecenoic acid, known as diffusible signal factor (DSF), induces callose deposition and cell death in *Arabidopsis*, *N. benthamiana* and rice [107]. Those examples indicate that plants could also be able to detect CDPs as QS molecules and react with different physiological changes. The plant dependent specificity in recognition could also include a receptor-mediated signaling.

4.2 What makes the activity

The structure of maculosin has two sides, a phenol ring as part of the amino acid tyrosine and a 2,5-diketopiperazine ring formed by the condensation with proline

(Fig. 3.19 (1)). In early studies, Park and Strobel [81] first suggested the 2,5-diketopiperazine moiety as binding part of maculosin. In this study a potential receptor or target was explored with affinity chromatography. In two experiments, both sides of the molecule were coupled to sepharose. The authors found ribulose-1,5-bisphosphat-carboxylase-oxygenase (RuBisCo) as protein with the highest binding affinity to the 2,5-diketopiperazine ring part of molecule and concluded this moiety as active side of maculosin. Indeed, many active 2,5-diketopiperazine contain the ring structure of prolin, which indicates the structural importance of this part. [108]. However, two years later, the same group hypothesized the phenol ring as important side for the phytotoxic activity [68]. By investigating different analogs of maculosin, they found the hydroxy group of the phenolic moiety as key feature for necrosis induction. The polarity and the thereby concomitant solubility in aqueous systems is important for the virulence.

The impact of single functional groups in terms of recognition and activation of basal immunity in plants is known. The bacterial medium-chain 3-hydroxy fatty acid elicits the receptor kinase LIPOOLIGOSACCHARIDE-SPECIFIC REDUCED ELICITATION (LORE). The free 3-hydroxyl group is thereby crucial for LORE-mediated immune activation [109]. The same can be observed with the group of 2,5-diketopipierazines. Structure-activity relationship studies of thaxtomins, a family of phytotoxins, revealed the 4-nitro indole fragment as well as the conformation as essential parts for the phytotoxicity [110]. Interestingly, additional functional groups in this phytotoxin family seem to influence crop selectivity [111].

In this work, five different cyclo dipeptides were tested in an ethylene induction assay (Fig.3.25). Cyclo(L-Phe-L-Pro) (2) is the closest homolog to maculosin, only lacking the hydroxyl group. Like maculosin, this molecule can influence plant development through auxin signaling [92]. Cyclo(L-Tyr-L-Trp) (3) shares the amino acid tyrosine compared to maculosin and holds a similar structure to the family of thaxtomins. Cyclo(L-Gly-L-Pro) (4), described as substance with antibiotic and phytotoxic properties [112] [113]. However, the classification as phytotoxin or antibiotic is rather an economic consideration [114] [115]. Cyclo(L-Trp-L-Pro)(5), also known

as Brevianamide F occurs as precursor of a variety of fungal prenylated alkaloids with diverse biological activities [116]. Cyclo(L-His-L-Pro)(6) is an endogenous mammalian signal molecule, acting in the central nervous system [93].

Taken together, all used peptides show biological relevance and share parts of the structure of maculosin. Despite that, none of them did induce ethylene production after treatment of the plants (summarized in Table 3.2). This indicates the whole molecular structure of maculosin as important for recognition by *S. pennellii*. Cyclo(L-His-L-Pro)(6) has a similar backbone as maculosin but due to the histidine an higher polarity. Cyclo(L-His-L-Pro) treatment did not lead to an ethylene response, which indicates a specific receptor rather than the polarity as major requirement.

This data also suggests one hydroxyl group as substantial for the ethylene inducing activity in *S. pennellii*, since cyclo(L-Phe-L-Pro) (2) did not activate immunity. The functional group could also explain the crop selectivity as it also the case for some thaxtomins. However, the few examples of immunity activation in plants through maculosin compared to the maculosin producing organisms indicates the phytotoxicity not as main function of maculosin. A corresponding receptor or target from *C. stoebe* or *S. pennellii*, could lead to a better understanding of the function.

4.3 Unravelling the target of maculosin

Different targets of maculosin in spotted knapweed have been hypothesized. Park and Strobel [81] describes that maculosin inhibits the enzyme RuBisCo at least 20 % with 0.15 µmol, proposing RuBisCo as target of maculosin. With this assumption two questions arise, first: Why is the toxin specific to spotted knapweed when it targets an enzyme which exists in all plants? A specific toxin requires a specific target. Second: RuBisCo is essential for carbon dioxide fixation. Inhibition of this process should kill the plant, which is not the case for maculosin. Aside RuBisCo, the group also suggests a target at the plasma membrane [81]. In fact, phytotoxins are known to target components of the cell membranes like structural or transport

proteins or lipids as well as enzymes [101]. Still, the question of specificity in case of target located in the cell membrane remains.

Cell disruption caused by maculosin could explain the formation of necrotic lesions, as well as ethylene production. Such effects are also trigged through NEP1-like proteins (NLPs), a conserved class of pore forming toxins produced by many microbes [56]. Yet, NLPs are pathotoxins and stimulate immunity associated defenses and cell death in all dicotyledonous plants tested and act in much lower concentrations [117]. Classified as vivotoxin, maculosin can cause different symptoms, but does not kill the host in the end. Cell disruption seems therefore implausible.

However, the specificity of maculosin points to an active recognition through a specific plant receptor. The introgression line screen performed in the sub project of Lambrianna Logarnudi could locate the receptor or target to chromosome 7 of *S. pennellii*. The receptor analogue for maculosin perception could be a member of a new class of receptor proteins, necessary for cross communication between plants and microbes.

4.4 Reviewing the project

MAMPs and PTI inducing molecules can be found in pathogenic as well as non-pathogenic bacteria. In this work, a collection of 83 non-pathogenic bacteria was explored for a novel PTI triggering substance in tomato. Ethylene accumulation was used as stress indicating output. A promising active bacterial culture broth, was analyzed and purified. Finally maculosin could be identified as ethylene inducing substance and charaterized by comparison with structural derivates. A selection of different plants were examined for phenotypes similar to *S. pennellii*. A gene involved in the recognition process could be localized on chromosome 7 via screen of a mapping population.

The bacterial collection was also screened for ethylene inducing activity in *Arabidopsis*. This work was done by Tobias Reißer.

4.4.1 The Tomato model system

Tomato was used as model system for several reasons. First, according to the FAO (2021), tomato belongs to the five most grown vegetables in the world [118]. It is therefore a very important crop. Second, although a genomic prediction indicates an array of PRRs [119], only three receptors for bacterial-derived MAMPs are known until today. The receptors are FLS2, FLS3 and CORE. This suggests an high potential for novel players in PTI signaling. Finally, Eshed and Zamir [75] created a mapping population between *S. pennellii* and *S. lycopersicum* M82. Upon treatment with a novel ligand, a forward genetic screen allows to trace a corresponding receptor back to the chromosome location.

4.4.2 The ethylene bioassay

An ethylene response from the plants´ side displays either a direct recognition i.e. by PRRs or indirect recognition of DAMPs through molecules which disrupt the cell integrity. To elicit the plants in the first performed screen, a crude sample, supernatant or cell extract, was added in different concentrations to the prepared

plant leaves. A bacterial culture is a very complex system from the chemical point of view, since countless proteins, peptides and small molecules of different classes are present. With almost 650 RLKs, which are predicted for the tomato genome [119], ethylene induction through multiple immunoactive substances is supposable. Although not all RLKs are PRRs involved in plant immunity (257 RLKs were predicted as LRR-RLKs), there is still a high potential for physiological alterations, followed by activation of PTI and ethylene production after treatment with a crude bacterial broth. When multiple defense elicitors act together, no statement about amount or potency can be made by evaluating the amount of ethylene. Beside that, the induction of ethylene is unspecific, in a sense that it is not restricted to stimulating processes occurring on the plasma membrane. No information about the mode of action is included, like for example from ROS burst, which is triggered presumably on the plasma membrane. Furthermore, ethylene production is not restricted to biotic stress, since high concentrations of salt could increase the osmotic pressure, which also leads to an activation of ethylene signaling [120]. However, an ethylene assay is fast in execution and compared to other assays less accident-sensitive.

4.4.3 Soil bacteria

Table 3.1 displays 14 strains which exhibited ethylene inducing qualities in *S. pennellii*. Although MAMPs often are body-derived structures of microbes i.e. bacterial-derived flagellin or fungal chitin, a lot of elicitors are known to be secreted. Among others, this group covers cell wall degrading enzymes [121], siderophores [122], harpins [123] and toxins [124]. Ethylene accumulation after treatment with a cell free supernatant is thus not surprising.

Rhodanobacter

Strain 1B4 (Table 3.1) is a Gram-negative and non-motile *Rhodanobacter* bacterium, which belongs to the class of gammaproteobacteria. SEM pictures (Fig. 3.4) show hair-like fimbria on the bacterial surface. Fimbria are proteins which allow

bacteria to stick to the surface, to remain at a favorable location [125]. Subunits of this proteins are proposed to be highly conserved, which makes them to possible PRR-targets [126].

On agar plates, *Rhodanobacter* first forms yellow pigmented colonies and in later stages a closed yellow biofilm. Yellow pigments indicate chromophores produced by the strain. Chromophores are known to have manifold functions, e.g. protection from damaging effects of light and oxygen [127]. They can also indicate the production of pyoverdines, a class of siderophores necessary for iron acquisition [128].

A biofilm formation involves the secretion of exopolysaccharides, an external digestive system. This matrix contains extracellular enzymes, nucleic acids, lipids and other biopolymers and bears a high potential for elicitors [129].

Fimbriae, siderophores and exopolysaccharides are possible PTI inducers. However, the *Rhodanobacter* cell extract as well as the cells itself did not induce ethylene accumulation in *S. pennellii* (Fig.3.2), which excludes all of those compounds.

Ensifer

Strain 2G2 (Table 3.1) belongs the genus *Ensifer* as part of the class alphaproteobacteria. This genus is also described as nitrogen-fixing rhizobacteria [130]. Like *Rhodanobacter*, the cell extract did not induce ethylene accumulation in *S. pennellii* [84], which points to a secreted elicitor. On agar plates *Ensifer* showed white colonies and a biofilm formation in a later stage. Unlike the *Rhodanobacter* activity, a purification with ion exchange chromatography was possible. This indicates an elicitor different from *Rhodanobacter*, since the size/charge ratio is different.

4.4.4 Diverse purification methods for versatile compound qualities

Most MAMPs and DAMPS were identified after purification from a culture extract [77]. Purification methods utilize physical and chemical properties of the analyte of interests to separate it from the rest. Conversely, a successful purification step

reveals properties of the analyte itself e.g. a solvent extraction reveals information about the substance polarity.

Common purification methods are fractionated protein precipitation, ion exchange chromatography, HPLC, and for concentrated samples size exclusion chormatography. The opportunities are numerous. In this work a hydrophobic polymeric resin was also successfully included. High resolution mass spectrometrical analysis revealed the mass and enabled the calculation of the molecular formula. Often proteins are to big for direct mass analysis and have to be digested beforehand. The generated peptide stings have to be recomposed afterwards. NMR experiments as well as infrared spectroscopy elucidate structural information but are also not suitable for proteins.

4.5 Different methods for PRR identification

After elicitor identification, different approaches are known to find the corresponding receptor [131].

4.5.1 Forward genetic screen

A successful strategy to identify PRRs is the forward genetic screen. Two parents with different phenotypic traits were used to create a mapping population. The population screen leads to the location of the trait of interest. Transient expression allows the correlation between a phenotype and a gene. The parasitic pattern recognizing receptor CuRe1 was identified with a forward genetic approach [132]. The same mapping population was used in this work to locate a gene which is involved in PTI after maculosin treatment.

With the mapping population, a receptor identification could also be achieved by testing the bacterial selection on a single introgression line instead the whole mapping population. As for the other strategy, the requirement is a different phenotype between the parental plants. As soon as the IL exhibits ethylene accumulation, a receptor location is found without knowledge of the ligand. Another advantage of this approach would be less plants which have to be compared and therefore less signal variation.

4.5.2 Reverese genetics

The reverse genetic approach leads from the gene to the phenotype and therefore requires the complete sequenced genome of the interested organism. Mutations of a single gene of interest as well as of a whole gene family can be explored. The effect in development and behavior can be traced back. This strategy was successfully applied for identification of EFR receptor in *A. thaliana* [131].

4.5.3 Biochemical approach

The high specificity between receptor and ligand can be utilized for receptor purification. An immobilized ligand can be used for affinity purification of the corresponding receptor. Also radioisotope labeling is a useful biochemical strategy to detect binding receptors. The successful implementation led to several pattern recognition receptors, e.g. PEPR1 in *A. thaliana*, *S. lycopersicum* and *Zea mays* [133]. However, both biochemical approaches are more difficult in their procedures, compared to the genetic strategies [131].

5 Appendix

The protein translation intiation facter 1 (IF1) is a known elicitor in *Arabidopsis thaliana*, with the corresponding patter recognition receptor RLP32. IF1 induces ethylene production in the tomato *Solanum lycopersicum* M82, which suggests a respective receptor in this plant. The tomato *Solanum pennellii* however does not respond to IF1 treatment. A foward genetic screen, using a genetic mapping population, with M82 background and *S. pennellii* insertions can therefore be used to find the corresponding IF1 receptor in tomato [134].

5.0.1 The IF1 corresponding receptor in *S. lycopersicum* M82

In an initial screen Dr. Katja Fröhlich could narrow down the population to 4 introgression lines (ILs), namely IL 7-4, IL 7-5, IL 11-4 and IL 12-2. An ethylene induction assay was performed with the same plants to confirm one of this introgression lines as potential receptor location, Fig. 5.1. *S. pennellii* and M82 were used as controls.

Since M82 is reacting to IF1 and *S. pennellii* is not, the ILs which do not respond upon IF1 treatment could lead to the IF1 receptor location. No ethylene was elicited in IL 7-4 and IL 7-5. As shown in the graphical map of this chromosome

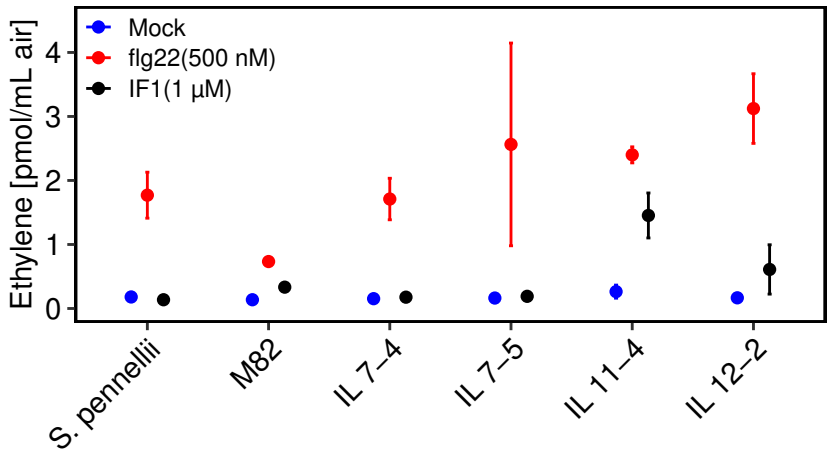

Figure 5.1: Ethylene accumulation of the introgression lines IL 7-4, IL 7-5, IL 11-4 and IL 12-2 after IF1 treatment (black). The experiment based on the work of Dr. Katja Fröhlich. Every dot represents the average of 3 replicats +/- S.D.. Plant leaf pieces were treated for 4 h. The experiment was repeated three times.

7 (Fig. 3.28), the insertions are overlapping, which suggests the receptor on IL 7-5. For further localisation, the backcross IL 7-5-5 was ordered and provided by the Tomato Genetic Resource Center of the UC Davis [135]. IL 7-5-5 was also tested for IF1 dependent ethylene accumulation, Fig. 5.2.

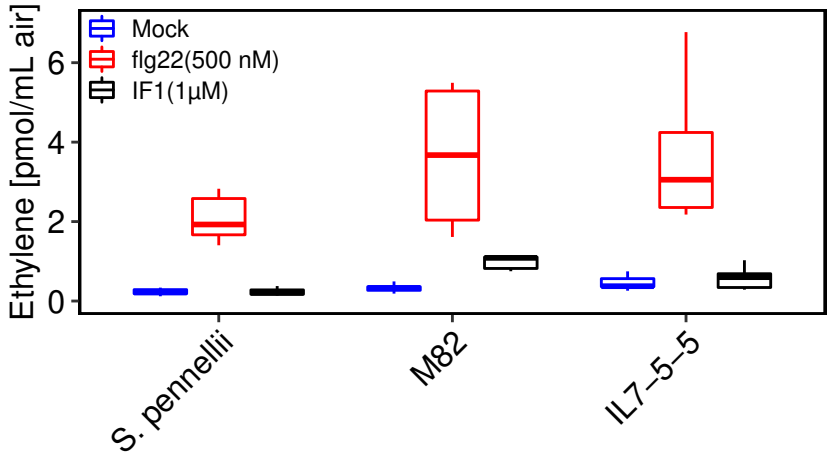

Figure 5.2: Ethylene production of IL 7-5-5 after IF1 treatment (black). The boxplot represents 9 independent experiments +/- S.D.. Plant leaf pieces were treated for 4 h. *S. pennellii* and M82 were used as controls.

Compared to the mock control (blue), IL 7-5-5 does not respond to IF1 treatment. This indicates the IF1 receptor located on this part of chromosome 7.

IF1 receptor candidates

Fig.3.28 also provides SNP markers flanking the region of the insertion 7-5-5, namely snp_37065(15) and snp_37030(26). With those markers, the region of interest could be analysed with the Solgenomics.net webside. The region contains around 1.5 billion base pairs (bp) and includes four RLKs:

- Solyc07g065860.3.1 (Receptor protein kinase, 3710 bp, 130 kDa), candidate 1.
- Solyc07g066230.4.1 (Receptor-like protein kinase, 3800 bp, 118 kDa), candidate 2.
- Solyc07g065240.4.1 (Receptor-like kinase, 1785 bp, 64 kDa), candidate 3.
- Solyc07g066360.1.1 (Proline-rich receptor-like protein kinase, 246 bp), candidate 4 .

Receptor candidates cloning procedure

Candidate 4 seemed to be too small for a plasma membrane receptor and was therefore excluded. Candidate 1-3 were synthesized (GenScript Biotech, Netherlands) and cloned using the Gateway system (Gateway Cloning Protocol, ThermoFisher Scientific). A Gateway entry clone was created using the BP reaction (BP Clonase II enzyme mix, ThermoFisher Scientific) with the competent *Escherichia coli* strain DH5α. The transformation to the destination vector was done with the LR reaction (LR Clonase II enzyme mix, ThermoFischer Scientific). The destination vector was then transformed into the competent cells of *Agrobacterium tumefaciens* strain GV3101, using electroporation, 1500 V. Selection was done with different antibiotics, table 5.2 (antibiotics were gathered after vector/strain specific resistance). Colonies grown on agar plates containing selective antibiotics were transferred into 3 mL of liquid LB medium, with the same antibiotics. The cells were incubated over night at 28 °C and 200 rpm. After separation (5000 rpm, 5 min), the cells were resuspended in MMA buffer with OD = 0.1. The obtained solution was infiltrated into four weeks old *Nicotiana benthamiana* leaves.

Primers: The pDONR Vector has additional sequences in front of the primer sequence. FW: GGGGACAAGTTTGTACAAAAAAGCAGGCTTC, REV: GGGGACCACTTTGTACAAGAAAGCTGGGTC.

Table 5.1: Primers used to clone the receptor candidates 1- 3.

Identifier	Sequence
Candi1_F1	ATGAGTCATAAAAGATGCCATGAA
Candi1_F2	CCTCAGTTGAGTTTCCACCCT
Candi1_F3	TTGCAGGAACTTGATATGGCTAG
Candi1_R	CGGTTCCCTTTCTTGCGATTC
Candi2_F1	ATGCTGGCTCCTTCAACATATC
Candi2_F2	GTCCATTACAGTTATTGACTTG
Candi2_F3	CAGGTGATATACCTAAAGAGTTG
Candi2_R	TTTGGTGATAGAGTTATCCGAAAA
Candi3_F1	ATGGACAATCTTCTCAAGTTCAT
Candi3_F2	GTGTGTGACACTGAAGAGAAAAG
Candi3_R	AAGGGCATAAACATGCTTCATTG

Medium and buffer

- LB medium: 10 g/L Bacto tryptone, 5 g/L Yeast extract, 5 g/L NaCl, pH 7.0.
- MMA buffer (50 mL): 1mL 0.5 M MES buffer (pH 5.7), 0.5 mL 1 M $MgCl_2$, 50 µL 150 mM Acetosyringon, H_2O.
- TBST buffer: 20 mM TRIS, 150 mM NaCl, pH 7.5, 0.1 % (v/v) Tween-20.

Vectors and antibiotics

- Vectors: pDONR207, pB7FWG2 (gfp), pGWB14 (ha), pGWB20 (myc).
- Antibiotics: Gentamycin (40 µg/mL), Rifampicin (100 µg/mL), Spectinomycin (100 µg/mL), Kanamycin (50 µg/mL).

PCR program

Table 5.2: Overview of time, temperature and cycles.

Time [min]	Temperature [°C]	Cycles
5:00	95	1
0:30	94	30
0:30	58	
1:30	72	
5:00	72	1
-	10	1

Antibodies:

- Primary antibodies: α-gfp, rabbit (Sicgen), α-myc, rabbit (Merck), α-ha, mouse (Merck).
- Secondary antibodies: α-rabbit (IgG), α-mouse (IgG), both purchased from Merck.

Western blot and immune induction assay

To verify whether the transformed receptor proteins with the different tags were expressed, a western plot was performed, Fig. 5.3. Approximately 30 mg grained leaf powder were mixed with 70 µL 2 x SDS loading buffer and boiled at 95 °C for 10 min. The remaining solid were spun down (14 000 rpm, 10 min). 15 µL of the remaining liquid were load into a 8 % SDS PAGE. The western blot was done with 100 mA for 1 h 15 min. Blocking was done with TBST buffer containing 5 % milk (Merck) over 1 h. The primary antibody, diluted in TBST buffer containing 5 % milk, was added. After 1 h, the primary antibody was removed and the blot was washed (3 x 10 min). The secondary antibody, also diluted in TBST buffer containing 5 % milk, was added and incubated for 1 h, followed by 3 x washing steps. A freshly prepared development solution, containing 186 µL Asssay B, 10 µL Tropix Nitro-Block II and 4 µL CDP-Stark, was added and the blot was recorded under a CCD camera. The *Agrobacterium* containing the receptor candidate 3 did not grew in this experiment. Except candidate 1 (α-myc), no protein was expressed, including

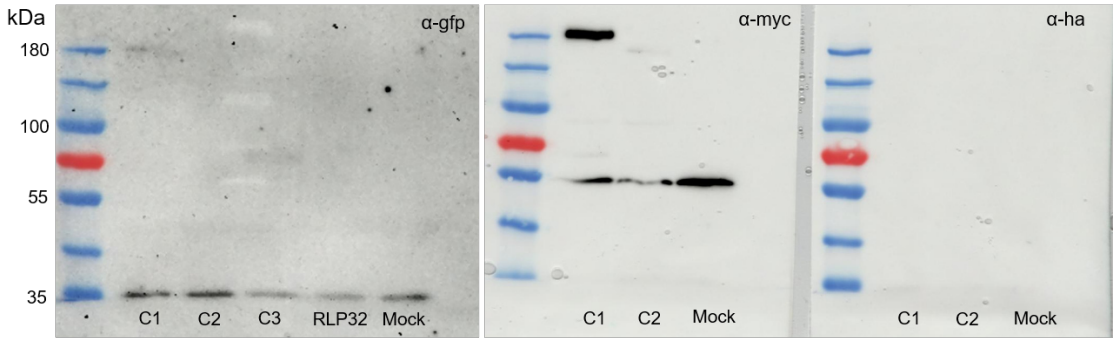

Figure 5.3: Western blot of the transformed IF1 receptor candidates in *N. benthamiana*. C1: Candidate 1, C2: Candidate 2, C3: Candidate 3 with used tags. RLP32 as used as positiv control.

the positive control. However, the expressed receptor was tested for ethylene production upon IF1 treatment, Fig. 5.4.

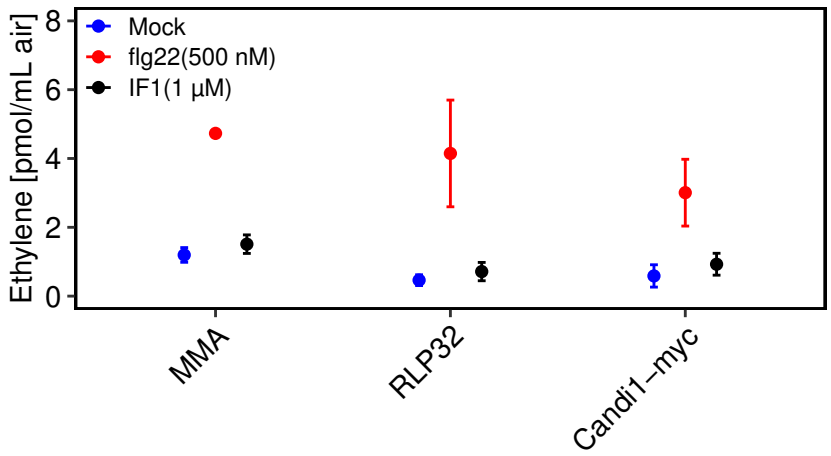

Figure 5.4: IF1 induced ethylene production in *N. benthamiana* after infiltration with *A. tumefaciens* carrying plasmids with RLP32 and receptor candidate Candi1 myc tagged, respectively. MMA buffer was infiltrated as control.

No enhanced ethylene production could be detected. Since a tag can also influence the receptor binding activity, only candidate 1 containing the myc-tag can be excluded as IF1 receptor after this experiment. This candidate could still be functional with a different tag or even without a tag. Though, an assumption of a classical receptor is fundamental for this approach. A different perception system could also be possible.

Bibliography

[1] United Nations. "World population prospects 2019: highlights". In: *Department of Economic and Social Affairs, Population Division* (2019).

[2] F.A.O.U. Nations et al. *The State of Food Security and Nutrition in the World 2021: Transforming food systems for food security, improved nutrition and affordable healthy diets for all*. The State of Food Security and Nutrition in the World (SOFI). FOOD & AGRICULTURE ORGN, 2021.

[3] Pamela C Ronald and Raoul W Adamchak. *Tomorrow's table: organic farming, genetics, and the future of food*. Oxford University Press, 2018.

[4] Mandeep Singh Hunjan and Jagjeet Singh Lore. "Climate Change: Impact on Plant Pathogens, Diseases, and Their Management". In: *Crop Protection Under Changing Climate*. Ed. by Khawar Jabran, Singarayer Florentine, and Bhagirath Singh Chauhan. Cham: Springer International Publishing, 2020, pp. 85–100.

[5] Amy Molotoks, Pete Smith, and Terence P. Dawson. "Impacts of land use, population, and climate change on global food security". In: *Food and Energy Security* 10.1 (Nov. 2020).

[6] Andrea A Gust, Frédéric Brunner, and Thorsten Nürnberger. "Biotechnological concepts for improving plant innate immunity". In: *Current Opinion in Biotechnology* 21.2 (2010). Food biotechnology – Plant biotechnology, pp. 204–210.

[7] Syed Adeel Zafar et al. "Engineering abiotic stress tolerance via CRISPR/Cas-mediated genome editing". In: *Journal of Experimental Botany* 71.2 (Oct. 2019), pp. 470–479.

[8] Ruslan Medzhitov and Charles A Janeway. "An ancient system of host defense". In: *Current Opinion in Immunology* 10.1 (1998), pp. 12–15.

[9] Frederick M Ausubel. "Are innate immune signaling pathways in plants and animals conserved?" In: *Nature immunology* 6.10 (2005), pp. 973–979.

[10] Delphine Chinchilla et al. "The Arabidopsis receptor kinase FLS2 binds flg22 and determines the specificity of flagellin perception". In: *The Plant Cell* 18.2 (2006), pp. 465–476.

[11] Thomas Boller. "Chemoperception of microbial signals in plant cells". In: *Annual review of plant biology* 46.1 (1995), pp. 189–214.

[12] Wei-Lin Wan et al. "Plant cell surface immune receptor complex signaling". In: *Current Opinion in Plant Biology* 50 (2019). Biotic interactions, pp. 18–28.

[13] Thomas WH Liebrand, Harrold A van den Burg, and Matthieu HAJ Joosten. "Two for all: receptor-associated kinases SOBIR1 and BAK1". In: *Trends in plant science* 19.2 (2014), pp. 123–132.

[14] Aranka M Van Der Burgh et al. “Kinase activity of SOBIR1 and BAK1 is required for immune signalling”. In: *Molecular plant pathology* 20.3 (2019), pp. 410–422.

[15] Jean Bigeard, Jean Colcombet, and Heribert Hirt. “Signaling Mechanisms in Pattern-Triggered Immunity (PTI)”. In: *Molecular Plant* 8.4 (2015). Cell Signaling, pp. 521–539.

[16] Pierre Buscaill et al. “Glycosidase and glycan polymorphism control hydrolytic release of immunogenic flagellin peptides”. In: *Science* 364.6436 (2019), eaav0748.

[17] Leighton Pritchard and Paul Birch. “A systems biology perspective on plant–microbe interactions: Biochemical and structural targets of pathogen effectors”. In: *Plant Science* 180.4 (2011), pp. 584–603.

[18] David Mackey et al. “RIN4 interacts with Pseudomonas syringae type III effector molecules and is required for RPM1-mediated resistance in Arabidopsis”. In: *Cell* 108.6 (2002), pp. 743–754.

[19] Laurent Deslandes and Susana Rivas. “Catch me if you can: bacterial effectors and plant targets”. In: *Trends in Plant Science* 17.11 (2012), pp. 644–655.

[20] Jeffery L Dangl and Jonathan DG Jones. “Plant pathogens and integrated defence responses to infection”. In: *nature* 411.6839 (2001), pp. 826–833.

[21] Ksenia V. Krasileva, Douglas Dahlbeck, and Brian J. Staskawicz. “Activation of an Arabidopsis Resistance Protein Is Specified by the in Planta Association of Its Leucine-Rich Repeat Domain with the Cognate Oomycete Effector ”. In: *The Plant Cell* 22.7 (July 2010), pp. 2444–2458.

[22] Erik A Van Der Biezen and Jonathan DG Jones. “Plant disease-resistance proteins and the gene-for-gene concept”. In: *Trends in biochemical sciences* 23.12 (1998), pp. 454–456.

[23] Jonathan D. G. Jones and Jeffery L. Dangl. “The plant immune system”. In: *Nature* 444.7117 (2006), pp. 323–329.

[24] Susana Rivas and Colwyn M Thomas. “Molecular interactions between tomato and the leaf mold pathogen Cladosporium fulvum”. In: *Annu. Rev. Phytopathol.* 43 (2005), pp. 395–436.

[25] Melvin D Bolton et al. “The novel Cladosporium fulvum lysin motif effector Ecp6 is a virulence factor with orthologues in other fungal species”. In: *Molecular microbiology* 69.1 (2008), pp. 119–136.

[26] Ronnie De Jonge and Bart PHJ Thomma. “Fungal LysM effectors: extinguishers of host immunity?” In: *Trends in microbiology* 17.4 (2009), pp. 151–157.

[27] Bart P.H.J. Thomma, Thorsten Nürnberger, and Matthieu H.A.J. Joosten. “Of PAMPs and Effectors: The Blurred PTI-ETI Dichotomy”. In: *The Plant Cell* 23.1 (Jan. 2011), pp. 4–15.

[28] Vivianne GAA Vleeshouwers and Richard P Oliver. “Effectors as tools in disease resistance breeding against biotrophic, hemibiotrophic, and necrotrophic plant pathogens”. In: *Molecular plant-microbe interactions* 27.3 (2014), pp. 196–206.

[29] Thomas Boller and Georg Felix. “A Renaissance of Elicitors: Perception of Microbe-Associated Molecular Patterns and Danger Signals by Pattern-Recognition Receptors”. In: *Annual Review of Plant Biology* 60.1 (2009). PMID: 19400727, pp. 379–406.

[30] A Gust, R Pruitt, and T Nürnberger. "Sensing Danger: Key to Activating Plant Immunity". In: *Trends Plant Sci* 22.9 (Aug. 2, 2017), pp. 779–791.

[31] Corné MJ Pieterse et al. "Networking by small-molecule hormones in plant immunity". In: *Nature chemical biology* 5.5 (2009), pp. 308–316.

[32] Bruno Pok Man Ngou et al. "Mutual potentiation of plant immunity by cell-surface and intracellular receptors". In: *Nature* 592.7852 (2021), pp. 110–115.

[33] Minhang Yuan et al. "Pattern-recognition receptors are required for NLR-mediated plant immunity". In: *Nature* 592.7852 (2021), pp. 105–109.

[34] Rory N. Pruitt et al. "The EDS1-PAD4-ADR1 node mediates Arabidopsis pattern-triggered immunity". In: *Nature* 598.7881 (2021), pp. 495–499.

[35] Melanie Morales and Sergi Munné-Bosch. "Oxidative stress: a master regulator of plant trade-offs?" In: *Trends in plant science* 21.12 (2016), pp. 996–999.

[36] Yuelin Zhang et al. "A gain-of-function mutation in a plant disease resistance gene leads to constitutive activation of downstream signal transduction pathways in suppressor of npr1-1, constitutive 1". In: *The Plant Cell* 15.11 (2003), pp. 2636–2646.

[37] Rowan Van Wersch, Xin Li, and Yuelin Zhang. "Mighty dwarfs: Arabidopsis autoimmune mutants and their usages in genetic dissection of plant immunity". In: *Frontiers in plant science* 7 (2016), p. 1717.

[38] Francisco Llorente et al. "ERECTA receptor-like kinase and heterotrimeric G protein from Arabidopsis are required for resistance to the necrotrophic fungus Plectosphaerella cucumerina". In: *The Plant Journal* 43.2 (2005), pp. 165–180.

[39] Polly Matzinger. "Friendly and dangerous signals: is the tissue in control?" In: *Nature immunology* 8.1 (2007), pp. 11–13.

[40] Gregory Pearce et al. "A polypeptide from tomato leaves induces wound-inducible proteinase inhibitor proteins". In: *Science* 253.5022 (1991), pp. 895–897.

[41] Yube Yamaguchi and Alisa Huffaker. "Endogenous peptide elicitors in higher plants". In: *Current opinion in plant biology* 14.4 (2011), pp. 351–357.

[42] Alisa Huffaker, Nicole J Dafoe, and Eric A Schmelz. "ZmPep1, an ortholog of Arabidopsis elicitor peptide 1, regulates maize innate immunity and enhances disease resistance". In: *Plant physiology* 155.3 (2011), pp. 1325–1338.

[43] Russell E Vance, Ralph R Isberg, and Daniel A Portnoy. "Patterns of pathogenesis: discrimination of pathogenic and nonpathogenic microbes by the innate immune system". In: *Cell host & microbe* 6.1 (2009), pp. 10–21.

[44] Leendert C van Loon, Bart PJ Geraats, and Huub JM Linthorst. "Ethylene as a modulator of disease resistance in plants". In: *Trends in plant science* 11.4 (2006), pp. 184–191.

[45] Martin De Vos et al. "Signal signature and transcriptome changes of Arabidopsis during pathogen and insect attack". In: *Molecular plant-microbe interactions* 18.9 (2005), pp. 923–937.

[46] Jane Glazebrook. "Contrasting mechanisms of defense against biotrophic and necrotrophic pathogens". In: *Annu. Rev. Phytopathol.* 43 (2005), pp. 205–227.

[47] Gregg A Howe. "Jasmonates as signals in the wound response". In: *Journal of Plant Growth Regulation* 23.3 (2004), pp. 223–237.

[48] Bart PHJ Thomma et al. "The complexity of disease signaling in Arabidopsis". In: *Current opinion in immunology* 13.1 (2001), pp. 63–68.

[49] Leendert C van Loon, Martijn Rep, Corné MJ Pieterse, et al. "Significance of inducible defense-related proteins in infected plants". In: *Annual review of phytopathology* 44 (2006), pp. 135–162.

[50] T Nürnberger et al. "Innate immunity in plants and animals: striking similarities and obvious differences". In: *Immunol Rev* 198 (Apr. 2004), pp. 249–266.

[51] Corné MJ Pieterse et al. "Rhizobacteria-mediated induced systemic resistance (ISR) in Arabidopsis requires sensitivity to jasmonate and ethylene but is not accompanied by an increase in their production". In: *Physiological and molecular plant pathology* 57.3 (2000), pp. 123–134.

[52] Stijn Spaepen, Jos Vanderleyden, and Roseline Remans. "Indole-3-acetic acid in microbial and microorganism-plant signaling". In: *FEMS microbiology reviews* 31.4 (2007), pp. 425–448.

[53] Tesfaye Mengiste et al. "Plant immunity to necrotrophs". In: *Annual review of phytopathology* 50.1 (2012), pp. 267–294.

[54] M Soledade C Pedras and Pearson WK Ahiahonu. "Phytotoxin production and phytoalexin elicitation by the phytopathogenic fungus Sclerotinia sclerotiorum". In: *Journal of Chemical Ecology* 30.11 (2004), pp. 2163–2179.

[55] Bryan A Bailey. "Purification of a protein from culture filtrates of Fusarium oxysporum that induces ethylene and necrosis in leaves of Erythroxylum coca". In: *Phytopathology* 85.10 (1995), pp. 1250–1255.

[56] Isabell Küfner et al. "Cytolytic toxins as triggers of plant immune response". In: *Plant signaling & behavior* 4.10 (2009), pp. 977–979.

[57] Jennifer M Lorang, Teresa A Sweat, and Thomas J Wolpert. "Plant disease susceptibility conferred by a "resistance" gene". In: *Proceedings of the National Academy of Sciences* 104.37 (2007), pp. 14861–14866.

[58] Nadine Möbius and Christian Hertweck. "Fungal phytotoxins as mediators of virulence". In: *Current Opinion in Plant Biology* 12.4 (2009), pp. 390–398.

[59] Stefka D Spassieva, Jonathan E Markham, and Jacques Hille. "The plant disease resistance gene Asc-1 prevents disruption of sphingolipid metabolism during AAL-toxin-induced programmed cell death". In: *The Plant Journal* 32.4 (2002), pp. 561–572.

[60] Margaret E Daub, Sonia Herrero, and Kuang-Ren Chung. "Photoactivated perylenequinone toxins in fungal pathogenesis of plants". In: *FEMS Microbiology Letters* 252.2 (2005), pp. 197–206.

[61] CJ Arntzen. "Inhibition of photophosphorylation by tentoxin, a cyclic tetrapeptide". In: *Biochimica et Biophysica Acta (BBA)-Bioenergetics* 283.3 (1972), pp. 539–542.

[62] Gavin Reineke et al. "Indole-3-acetic acid (IAA) biosynthesis in the smut fungus Ustilago maydis and its relevance for increased IAA levels in infected tissue and host tumour formation". In: *Molecular plant pathology* 9.3 (2008), pp. 339–355.

[63] Teresa A Sweat and Thomas J Wolpert. "Thioredoxin h 5 is required for victorin sensitivity mediated by a CC-NBS-LRR gene in Arabidopsis". In: *The Plant Cell* 19.2 (2007), pp. 673–687.

[64] Daisuke Masuda et al. "Phytotoxic effects of trichothecenes on the growth and morphology of Arabidopsis thaliana". In: *Journal of Experimental Botany* 58.7 (2007), pp. 1617–1626.

[65] Franck E Dayan, Daniel K Owens, and Stephen O Duke. "Rationale for a natural products approach to herbicide discovery". In: *Pest management science* 68.4 (2012), pp. 519–528.

[66] Andrea C Stierle, John H Cardellina, and Gary A Strobel. "Maculosin, a host-specific phytotoxin for spotted knapweed from Alternaria alternata". In: *Proceedings of the National Academy of Sciences* 85.21 (1988), pp. 8008–8011.

[67] G Puopolo et al. "Lysobacter capsici AZ78 produces cyclo (l-Pro-l-Tyr), a 2, 5-diketopiperazine with toxic activity against sporangia of P hytophthora infestans and P lasmopara viticola". In: *Journal of applied microbiology* 117.4 (2014), pp. 1168–1180.

[68] Mikhail M Bobylev, Ludmila I Bobyleva, and Gary A Strobel. "Synthesis and bioactivity of analogs of maculosin, a host-specific phytotoxin produced by Alternaria alternata on spotted knapweed (Centaurea maculosa)". In: *Journal of agricultural and food chemistry* 44.12 (1996), pp. 3960–3964.

[69] Klaus Brilisauer et al. "Cyanobacterial antimetabolite 7-deoxy-sedoheptulose blocks the shikimate pathway to inhibit the growth of prototrophic organisms". In: *Nature communications* 10.1 (2019), pp. 1–11.

[70] Ulrich Karl LAEMMLI. "Cleavage of structural proteins during the assembly of the head of bacteriophage T4". In: *nature* 227.5259 (1970), pp. 680–685.

[71] Joseph Sambrook. *Molecular cloning: a laboratory manual/Joseph Sambrook, David W. Russell*. 2001.

[72] Hanh P Nguyen et al. "Methods to study PAMP-triggered immunity using tomato and Nicotiana benthamiana". In: *Molecular Plant-Microbe Interactions* 23.8 (2010), pp. 991–999.

[73] Ulrik Lyngs. *oxforddown: An Oxford University Thesis Template for R Markdown*. `https://github.com/ulyngs/oxforddown`. 2019.

[74] Yang Bai et al. "Functional overlap of the Arabidopsis leaf and root microbiota". In: *Nature* 528.7582 (2015), pp. 364–369.

[75] Y Eshed and D Zamir. "An introgression line population of Lycopersicon pennellii in the cultivated tomato enables the identification and fine mapping of yield-associated QTL." In: *Genetics* 141.3 (Nov. 1995), pp. 1147–1162.

[76] Thomas Meindl, Thomas Boller, and Georg Felix. "The Bacterial Elicitor Flagellin Activates Its Receptor in Tomato Cells According to the Address–Message Concept". In: *The Plant Cell* 12.9 (Dec. 2000), pp. 1783–1794.

[77] Freddy Boutrot and Cyril Zipfel. "Function, discovery, and exploitation of plant pattern recognition receptors for broad-spectrum disease resistance". In: *Annual review of phytopathology* 55 (2017), pp. 257–286.

[78] Katharina Mueller et al. “Contamination risks in work with synthetic peptides: flg22 as an example of a pirate in commercial peptide preparations”. In: *The plant cell* 24.8 (2012), pp. 3193–3197.

[79] Lei Wang et al. “The pattern-recognition receptor CORE of Solanaceae detects bacterial cold-shock protein”. In: *Nature plants* 2.12 (2016), pp. 1–9.

[80] Young Ho Nam et al. “Isolation and characterization of strain Rouxiella sp. S1S-2 producing antibacterial compound”. In: *The Microbiological Society of Korea* 56.2 (2020), pp. 152–159.

[81] Sang Ho Park and Gary A Strobel. “Cellular protein receptors of maculosin, a host specific phytotoxin of spotted knapweed (Centaurea maculosa L.)” In: *Biochimica et Biophysica Acta (BBA)-General Subjects* 1199.1 (1994), pp. 13–19.

[82] Silke Robatzek et al. “Molecular identification and characterization of the tomato flagellin receptor LeFLS2, an orthologue of Arabidopsis FLS2 exhibiting characteristically different perception specificities”. In: *Plant Molecular Biology* 64.5 (2007), pp. 539–547.

[83] Babita Paudel et al. “Maculosin, a non-toxic antioxidant compound isolated from Streptomyces sp. KTM18”. In: *Pharmaceutical biology* 59.1 (2021), pp. 931–934.

[84] Lambrianna Logarnudi. “Identification of Receptor-Elicitor Pairs in the Tomato Species Solanum pennellii”. In: *Bachelorthesis* (2021).

[85] Randy Ortiz-Castro et al. “Transkingdom signaling based on bacterial cyclodipeptides with auxin activity in plants”. In: *Proceedings of the National Academy of Sciences* 108.17 (2011), pp. 7253–7258.

[86] Xiaoqi Chen et al. “Cyclic dipeptides produced by fungus Eupenicillium brefeldianum HMP-F96 induced extracellular alkalinization and H2O2 production in tobacco cell suspensions”. In: *World Journal of Microbiology and Biotechnology* 31.1 (2015), pp. 247–253.

[87] Omar González et al. “Non-ribosomal peptide synthases from Pseudomonas aeruginosa play a role in cyclodipeptide biosynthesis, quorum-sensing regulation, and root development in a plant host”. In: *Microbial ecology* 73.3 (2017), pp. 616–629.

[88] Ahmed M Zaher et al. “Characterisation of the metabolites of an antibacterial endophyte Botryodiplodia theobromae Pat. of Dracaena draco L. by LC–MS/MS”. In: *Natural product research* 29.24 (2015), pp. 2275–2281.

[89] Giuliano Degrassi et al. “Plant Growth-Promoting Pseudomonas putida WCS358 Produces and Secretes Four Cyclic Dipeptides: Cross-Talk with Quorum Sensing Bacterial Sensors”. In: *Current Microbiology* 45.4 (2002), pp. 250–254.

[90] Saburo Tamura et al. “Isolation of several diketopiperazines from peptone”. In: *Agricultural and Biological Chemistry* 28.9 (1964), pp. 650–652.

[91] Kazuya Nakagawa, Kentaro Takada, and Nobutaka Imamura. “Probable novel MEP pathway inhibitor and its binding protein, IspG”. In: *Bioscience, biotechnology, and biochemistry* 77.7 (2013), pp. 1449–1454.

[92] Aurelio Ortiz and Estibaliz Sansinenea. “Cyclic dipeptides: secondary metabolites isolated from different microorganisms with diverse biological activities”. In: *Current Medicinal Chemistry* 24.25 (2017), pp. 2773–2780.

[93] Chandan Prasad. “Bioactive cyclic dipeptides”. In: *Peptides* 16.1 (1995), pp. 151–164.

[94] PJ Milne et al. “The biological activity of selected cyclic dipeptides”. In: *Journal of Pharmacy and Pharmacology* 50.12 (1998), pp. 1331–1337.

[95] Matthew TG Holden et al. “Quorum-sensing cross talk: isolation and chemical characterization of cyclic dipeptides from Pseudomonas aeruginosa and other gram-negative bacteria”. In: *Molecular microbiology* 33.6 (1999), pp. 1254–1266.

[96] Giuliano Degrassi et al. “Plant growth-promoting Pseudomonas putida WCS358 produces and secretes four cyclic dipeptides: cross-talk with quorum sensing bacterial sensors”. In: *Current microbiology* 45.4 (2002), pp. 250–254.

[97] Xiao-Jun Li et al. “Toxins from a symbiotic fungus, Leptographium qinlingensis associated with Dendroctonus armandi and their in vitro toxicities to Pinus armandi seedlings”. In: *European journal of plant pathology* 134.2 (2012), pp. 239–247.

[98] Sangluo Chen et al. “A rare diketopiperazine glycoside from marine-sourced Streptomyces sp. ZZ446”. In: *Natural Product Research* 34.7 (2020), pp. 1046–1050.

[99] Gamini S Jayatilake et al. “Metabolites from an Antarctic sponge-associated bacterium, Pseudomonas aeruginosa”. In: *Journal of Natural Products* 59.3 (1996), pp. 293–296.

[100] Luz Irina Calderon-Villalobos et al. “Auxin perception—structural insights”. In: *Cold Spring Harbor perspectives in biology* 2.7 (2010), a005546.

[101] AO Berestetskiy. “A review of fungal phytotoxins: from basic studies to practical use”. In: *Applied Biochemistry and Microbiology* 44.5 (2008), pp. 453–465.

[102] H-H Hoppe. “Pathogenicity of sirodesmin-deficient mutants of Phoma lingam”. In: *Journal of phytopathology* 147.3 (1999), pp. 169–173.

[103] Joseph W Kloepper et al. “Enhanced plant growth by siderophores produced by plant growth-promoting rhizobacteria”. In: *Nature* 286.5776 (1980), pp. 885–886.

[104] Hamid Meziane et al. “Determinants of Pseudomonas putida WCS358 involved in inducing systemic resistance in plants”. In: *Molecular Plant Pathology* 6.2 (2005), pp. 177–185.

[105] Ulrike Mathesius et al. “Extensive and specific responses of a eukaryote to bacterial quorum-sensing signals”. In: *Proceedings of the National Academy of Sciences* 100.3 (2003), pp. 1444–1449.

[106] Wolfgang D Bauer and Ulrike Mathesius. “Plant responses to bacterial quorum sensing signals”. In: *Current opinion in plant biology* 7.4 (2004), pp. 429–433.

[107] Akanksha Kakkar et al. “Xanthomonas campestris cell–cell signalling molecule DSF (diffusible signal factor) elicits innate immunity in plants and is suppressed by the exopolysaccharide xanthan”. In: *Journal of Experimental Botany* 66.21 (2015), pp. 6697–6714.

[108] Seth Clint Brauns et al. “Selected cyclic dipeptides inhibit cancer cell growth and induce apoptosis in HT-29 colon cancer cells”. In: *Anticancer research* 24.3A (2004), pp. 1713–1720.

[109] Alexander Kutschera et al. “Bacterial medium-chain 3-hydroxy fatty acid metabolites trigger immunity in Arabidopsis plants”. In: *Science* 364.6436 (2019), pp. 178–181.

[110] Russell R King et al. “Isolation and characterization of phytotoxins associated with Streptomyces scabies”. In: *Journal of the Chemical Society, Chemical Communications* 13 (1989), pp. 849–850.

[111] Hongbo Zhang et al. “Synthesis and biological evaluations of a series of thaxtomin analogues”. In: *Journal of agricultural and food chemistry* 63.14 (2015), pp. 3734–3741.

[112] Angel Trigos, Silvia Reyna, and Lourdes Cervantes. “Three diketopiperazines from the cultivated fungus Fusarium oxysporum”. In: *Natural Product Letters* 6.4 (1995), pp. 241–246.

[113] Shuo Tan et al. “Photosynthetic inhibition and oxidative stress to the toxic Phaeocystis globosa caused by a diketopiperazine isolated from products of algicidal bacterium metabolism”. In: *Journal of Microbiology* 54.5 (2016), pp. 364–375.

[114] OA Berestetskii and AV Borovkov. “Phytotoxic metabolites of soil penicillia”. In: *Mikrobiologicheskii zhurnal* (1979).

[115] H Oku and T Nakanishi. “A toxic metabolite from Ascochyta fabae having antibiotic activity”. In: *Phytopathology* 53.11 (1963), p. 1321.

[116] Alan D Borthwick. “2, 5-Diketopiperazines: synthesis, reactions, medicinal chemistry, and bioactive natural products”. In: *Chemical reviews* 112.7 (2012), pp. 3641–3716.

[117] Christian Ottmann et al. “A common toxin fold mediates microbial attack and plant defense”. In: *Proceedings of the National Academy of Sciences* 106.25 (2009), pp. 10359–10364.

[118] FAO. “Production: Crops and livestock products.” In: (2021).

[119] Tetsu Sakamoto et al. “The tomato RLK superfamily: phylogeny and functional predictions about the role of the LRRII-RLK subfamily in antiviral defense”. In: *BMC Plant Biology* 12.1 (2012), p. 229.

[120] Ruidang Quan et al. “EIN3 and SOS2 synergistically modulate plant salt tolerance”. In: *Scientific reports* 7.1 (2017), pp. 1–11.

[121] Yanan Ma et al. “Fungal cellulase is an elicitor but its enzymatic activity is not required for its elicitor activity”. In: *Molecular plant pathology* 16.1 (2015), pp. 14–26.

[122] M Leeman et al. “Iron availability affects induction of systemic resistance to Fusarium wilt of radish by Pseudomonas fluorescens”. In: *Phytopathology* 86.2 (1996), pp. 149–155.

[123] Zhong-Min Wei et al. “Harpin, elicitor of the hypersensitive response produced by the plant pathogen Erwinia amylovora”. In: *Science* 257.5066 (1992), pp. 85–88.

[124] Hannah Böhm et al. “A conserved peptide pattern from a widespread microbial virulence factor triggers pattern-induced immunity in Arabidopsis”. In: *PLoS pathogens* 10.11 (2014), e1004491.

[125] Martin Romantschuk. “Attachment of plant pathogenic bacteria to plant surfaces”. In: *Annual review of phytopathology* 30.1 (1992), pp. 225–243.

[126] Brian Dalrymple and John S Mattick. “An analysis of the organization and evolution of type 4 fimbrial (MePhe) subunit proteins”. In: *Journal of molecular evolution* 25.3 (1987), pp. 261–269.

[127] Maurice Moss. “Bacterial pigments”. In: *Microbiologist* 3.4 (2002), pp. 10–12.

[128] Jean-Marie Meyer. “Pyoverdines: pigments, siderophores and potential taxonomic markers of fluorescent Pseudomonas species”. In: *Archives of microbiology* 174.3 (2000), pp. 135–142.

[129] Hans-Curt Flemming and Jost Wingender. “The biofilm matrix”. In: *Nature reviews microbiology* 8.9 (2010), pp. 623–633.

[130] Miet Martens et al. “Advantages of multilocus sequence analysis for taxonomic studies: a case study using 10 housekeeping genes in the genus Ensifer (including former Sinorhizobium)”. In: *International journal of systematic and evolutionary microbiology* 58.1 (2008), pp. 200–214.

[131] Cyril Zipfel et al. “Perception of the bacterial PAMP EF-Tu by the receptor EFR restricts Agrobacterium-mediated transformation”. In: *Cell* 125.4 (2006), pp. 749–760.

[132] Volker Hegenauer et al. “Detection of the plant parasite Cuscuta reflexa by a tomato cell surface receptor”. In: *Science* 353.6298 (2016), pp. 478–481.

[133] Martina Lori et al. “Evolutionary divergence of the plant elicitor peptides (Peps) and their receptors: interfamily incompatibility of perception but compatibility of downstream signalling”. In: *Journal of experimental botany* 66.17 (2015), pp. 5315–5325.

[134] Katja Fröhlich. “Functional characterization of the immune receptro RLP32 and its ligand IF1”. In: *Dissertation* (2020).

[135] Itai Ofner et al. “Solanum pennellii backcross inbred lines (BIL s) link small genomic bins with tomato traits”. In: *The Plant Journal* 87.2 (2016), pp. 151–160.